Analysis and Impact of Shading Patterns on Single and Double Diode Solar Cells Using Different Materials

Author

MUHAMMAD KASHIF RIAZ

00000276403

Supervisor

DR. SAIF ULLAH AWAN

DEPARTMENT OF ELECTRICAL ENGINEERING

COLLEGE OF ELECTRICAL & MECHANICAL ENGINEERING

NATIONAL UNIVERSITY OF SCIENCES AND TECHNOLOGY

ISLAMABAD

August, 2022

Analysis and Impact of Shading Patterns on Single and Double Diode Solar Cells Using Different Materials

Author

MUHAMMAD KASHIF RIAZ

00000276403

A thesis submitted in partial fulfillment of the requirements for the degree of

MS Electrical Engineering

Thesis Supervisor:

DR. SAIF ULLAH AWAN

Thesis Supervisor's Signature: _____

DEPARTMENT OF ELECTRICAL ENGINEERING

COLLEGE OF ELECTRICAL & MECHANICAL ENGINEERING

NATIONAL UNIVERSITY OF SCIENCES AND TECHNOLOGY, ISLAMABAD

August, 2022

Declaration

I certify that this research work titled "Analysis and Impact of shading patterns on single and double diode solar cells using different materials*"* is my own work. The work has not been presented elsewhere for assessment. The material that has been used from other sources it has been properly acknowledged / referred.

Signature of Student

MUHAMMAD KASHIF RIAZ

00000276403

LANGUAGE CORRECTNESS CERTIFICATE

This thesis has been read by an English expert and is free of typing, syntax, semantic, grammatical and spelling mistakes. Thesis is also according to the format given by the university.

Signature of Student

MUHAMMAD KASHIF RIAZ

00000276403

Signature of Supervisor

COPYRIGHT STATEMENT

ACKNOWLEDGEMENTS

I would like to thank Allah (SWT) who has always showered his countless blessings on me.

A special thanks to my supervisor Dr. Saif ullah Awan for their tremendous supervision, and a very reliable encouragement throughout the course of this thesis. I wouldn't have been here today without his encouragement.

I would also like to thank Dr. Toasif Iqbal, Dr. Azhar ul Haq and Dr. Usman for being on my thesis Guidance and Examination Committee and for guidance.

I am also thankful to Sir Ihsan ullah Khalil for their support and encouragement from the very beginning of my master's program.

Finally, thanks to my parents who always encouraged and supported me whenever I was stuck or confused with the work.

I dedicate this thesis to

My Parents,

Sister & Brothers

Abstract

Adoption rate of Photovoltaic systems as a secondary source of energy is increasing sharply. Partial shadowing drastically decreases output PV power and shortens working lifetime. In this research work performance and efficiency of single and double diode solar cell models of different material such as Copper indium selenide (CIS), Cadmium telluride (CdTe), Copper Indium Gallium Selenide (CIGS), and Amorphous Silicon (a-Si) will be analyzed under different shading patterns. The novelty of this research work is analyzing the impact of different shadowing patterns on the output of PV arrays of single and double diode solar cell models made up of above-mentioned materials. This research shows the CIS has higher efficiency among all four materials due to its higher lab efficiency of 22.9%. This research will result in set of recommendations for adoption of specific PV system for different shadowing conditions.

Table of Contents

List of Figures

CHAPTER 1: INTRODUCTION

1.1 Introduction

As we see the impact of alternative energy, the project begins to explain the current state of energy. Energy is an issue that affects everyone in the world. Nowadays, in the world, especially in industrialized and developing countries, energy has become very important for all acquaintances and relatives. as a result, the demand for energy has been increasing dramatically in recent years.

Due to the atmospheric phenomenon, the impact on the environment, and also the increasing value of fossil fuel based energy sources, it becomes further much more rather more much greater the consumption of renewable energy and the more economical use of standard sources. The globe Resource Institute estimates that 61.4% of global greenhouse gas emissions come from energy consumption. So the answer to curbing these pollutants should include investments in renewables and energy efficiency so that energy can play its role in the economy without endangering the environment [1].

The increasing value of electricity as well as the increasing environmental impact the world is suffering from; alternative energy is also significantly accepted as one of the key solutions.

Solar energy is radiant, light and heat that returns from radiation. it is a renewable resource because the strategies used to transform alternative energy into electricity produce no smoke or pollutants. However, since the ability generated by this stock comes from daylight, it cannot be used all night and even on some days when the weather is completely cloudy, rainy, snowing, or other natural factors. alternative energy will be mainly divided into 2 mainly sources; will be used by the stellar thermal and Photovoltaic (PV) pathways for a number of applications. The analysis was focused on photovoltaics as part of alternative energy [2].

Solar electrical phenomenon modules area unit factory made of semiconductor materials and that they convert the energy coming from the sun into electrical energy and thus into electricity. The struggle on this field is increasing; in 2013, for the first time in more than a decade, it was the solar above all alternative renewable energy technologies in terms of the latest generation capacity installed, with an increase of 29% compared to 2012. Worldwide photovoltaic installations reached 1.8 GW in 2000 and 71.1 GW in 2011 with a quarter mile growth rate. This has a diode on state

wherever electricity from solar panels costs the maximum amount or is even cheaper than electricity purchased from the grid in sight.

However, alternative energy production still has some following problems: the conversion ability of the solar cells is lower, and also the output power of the PV has a good relationship with the irradiance and temperature.

Regardless of the above problems, one of the most important problems in the photovoltaic field is the impact of shading. Shaded conditions are usually unavoidable as a result of some elements of the electrical system receiving less daylight intensity due to many factors such as clouds, time of day, season or perhaps shadows from neighboring objects [3].

1.2 Photovoltaic cell

Meeting the world's evolving energy demand is probably the most notable. As the total number of people evolves and the expectations of daily comfort improve, the power consumption of the shoe increases. Today, a significant chunk of man-made energy comes from petroleum products, however tragically there are limited supplies of non-renewable energy sources, essential energy sources. The use of petroleum products causes environmental risks associated with a slight increase in unnatural weather variability as these assets are distributed per unit area. There is pressure must be forced to depend on advances that the area unit financially possible and harmless to the system. Energy from sources in light of a lot of current innovations, for example robust solid state electrical phenomenon gadgets have emerged as a typically economic supply of energy, naturally good and valuable whenever supplied on a massive scale. Energy primarily based on daylight in some structure is the source of primarily all energy in the world. All creatures and plants (living things) depend on the sun for warmth and food. Humans harness solar energy in a variety of ways. A standard of 125,000 TW of energy primarily based on the sun will hit the United States planet at any time. In this way, primarily daylight-based energy is good for the age of power because it is abundant, good, and possessive [4].

1.3 History of Solar cells

Energy plays a vital role in the mechanical and financial improvement of human beings. the greater part of the public relies on oil, coal and combustible gas to produce an outsized part of their energy needs, this amount of petroleum derivatives is of limited quality. the planet may also be running

out of non-renewable energy sources because it might end up being too expensive. the use of non-renewable energy sources also supplies harmful gases that cause unnatural weather changes and cause soil, air and water contamination.

As the population grows, the global interest in energy systematically increases, because energy is a convenient and superficial purpose of concern for humanized social orders. As a noteworthy important energy quality, hydrocarbons seriously save victims of area units with human public growth and high trend. Humanity seems headed for an energy emergency. Relocation should be initiated to support new energy sources for research and extremely used asset bases and to accommodate the current emergency [5]. Energy asset assets that consist mainly of wind, solar, hydropower, biomass, geothermal resources, hydrogen resources and ocean resources provide clean options for petroleum derivatives. they never run out and produce no contaminating or gas damaging substances.

Energy based primarily on the Sun is abundant, perfect, modest, a property, free of harmful side effects, available everywhere and a particularly attractive optional resource. the electric phenomenon impact is that direct transformation of solar energy into energy through electronic devices referred to as sun semiconductor cells(SC). SC are mainly composed of Si (Si), the leading well-known element on Earth, is absolutely easy and with no moving half to break down, it will work for a long time with (almost nothing) repairs and also add a shady climate.

In 1839, the French scientist Edmond Henri Becquerel first discovered the impact of the electrical phenomenon. Once he coordinated the daylight, he could see the tension build cathode in a solution while different things with a 2-metal cell terminals are placed in an extremely efficient arrangement. He saw the power age extended once granted to the light. In 1860, the French scientist August Mouchet lent the probability of a solar steam engine and subsequently he and Abel Pifre constructed it primary oil engine heated towards home. gift day allegorical dish authority's area unit models of it engine. William Grylls Adams and Richard Evans Day noted the effect of PV on antioxidants [6].

In 1880, Samuel P. Langly designed a light weight estimating device and named it the "Bolometer". The main solar cell (1% efficiency) from antioxidant plates appeared in 1838, designer was ripped scientist Charles Fritts, UN agency coated semiconductor Selenium with a really thin layer of gold forming the intersections. A progressive matter and in 1891 the Kemp equipage protected the equipment associated with daylight primarily on a water radiator. And the

number of different specialists and researchers who continue during this turn of events, Wilhelm Hallwachs discovered in 1904 that it was a mixture of copper and metal photosensitive.

Pure man of science Leden Czochralski supported the technique of developing individual jewelry of silicon in 1918, the inspiration for Si innovation on Boxing Day. The event was conducted by the congregation researcher at Bell Laboratories in the US. pp. (USA) wherever they created the most daylight primarily based cell with a four-dimensional change productivity in 1953. Reynolds developed Cadmium-Sulfide with comparable productivity at the same time. This upheaval of events and upgrade remains in the firing line, in addition, completely different ages and types of PV cells are currently being created.

1.4 Single Diode Model

The actual Photovoltaic (PV) board/module is also use as carrier of current as diode and resistor can be attached parallel to each other in the circuit as it is shown in the circuit below which is figure 1.

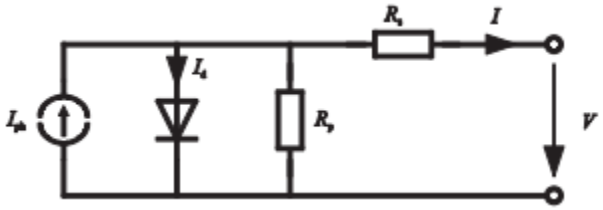

Figure 1: Basic model of single diode use in PV cells [7]

In this identical circuit, which is shown in above figure I_{ph} it shows as the generation of current which is produce during sunlight on a module referred to as the photocurrent. I_d is that the p-n junction flows as indicated by the physical condition. The characteristic impedance of the semiconductor, the opposition of the metal grid associating the individual PV cells within the plate, the association opposition and therefore measure of the interface impedance undeniably concentrated into the series opposition R_s . The opposition R_p in Fig. 1 models the natural shunts of the PV module.

1.5 Double Diode Model

The two-diode model (TDM) is obtained from the ODM by adding an additional diode in line with all existing diodes. This future diode models a recombination accident at the point of consumption. The equivalent TDM circuit is shown in Figure 2 below.

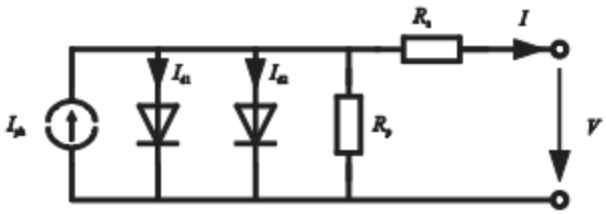

Figure 2 Basic model of Double diode use in PV cells [7]

1.6 Material used in shading patterns

The following four materials are used in the research to obtained the desired results which will be discuss later in the thesis in detail for both single diodes in the PV cells and double diode in the PV cells the materials remains the same in the process of obtaining results.

- Cadmium telluride (CdTe)
- Copper indium selenide (CIS)
- Copper indium gallium selenide (CIGS)
- Amorphous Silicone (a-Si)

Now we will give a little detail of the above materials used in this research

1.6.1 Cadmium telluride (CdTe)

CdTe incorporates a direct bandgap with 1.5eV associate best material for top proficiency with borderline expense. Its activity constant approximately equal to (~10^5/cm) is great, a layer thickness of a handful of micrometer is up to retain ~ ninetieth of the gauge photon. With a usually wonderful and high-proficiency of 19.6% is accounted for.

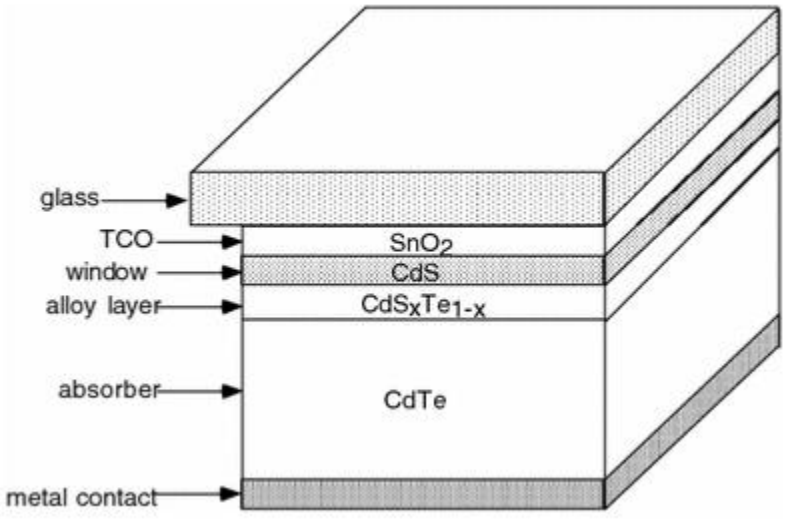

Figure 3: Basic structure of cadmium telluride cells [8]

1.6.2 Copper indium selenide (CIS)

CIS cells formed by a thin layer of CuInSe2 on plain glass or an adaptable metal substrate. The efficiency of CIS cells is 14% which is based on reliability of solar cell silicon. Because they have thin layer and that is why its cost effect is less than Si cells. These cells have an electrical circuit voltage of 5 volts DC and short output current 95 mA. The most extreme power is 3.9 V and 64 mA (0.25 watts).

1.6.3 Copper indium gallium selenide (CIGS)

Copper Indium Gallium Selenide (CIGS) can be used as a direct bandgap semiconductor that is useful for assembling cells. it is crystalline in nature and achieved a high treatment efficiency of 2.3% for 1-SUN and 21.5% under somewhat imaginary (14.05 SUN) daylight several times. Each of the results expressed here exploratory; in any case, our recreation results measure higher.

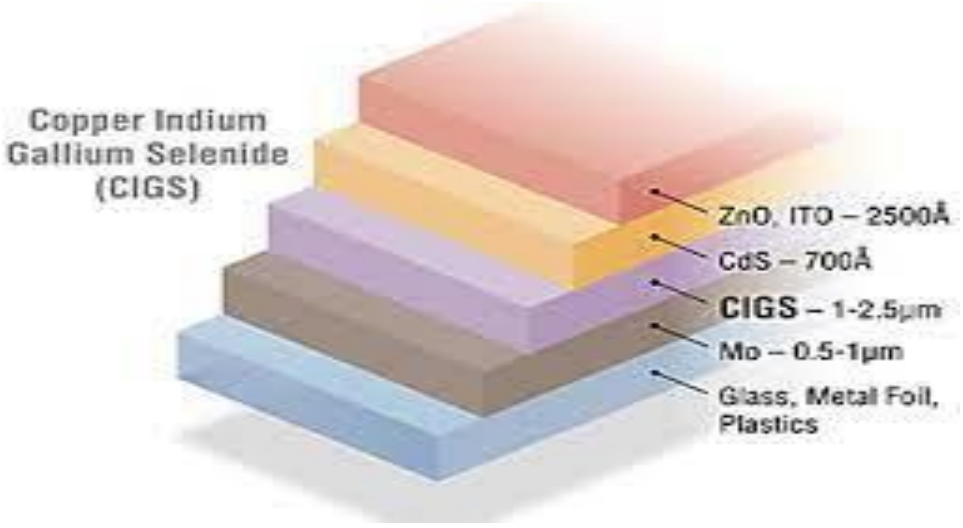

Figure 4:Basic structure of CIGS cells [8]

1.6.4 Amorphous Silicone (a-Si)

Amorphous silicon(a-Si) is an opaque allotropic variant of a semiconducting semiconductor. it is a high retention limit and thus can be used in solar cells mostly with small film thicknesses (typically a 100 timeless than pure silicon), less costly on material costs and creating implementation deficiencies caused by its equivalently low most extreme expertise in field, which ranges around 13%. In spite of their lower performance once contrasted with crystalline silicon semiconductor (c-Si) cells. a-Si it can be operated at extremely low temperature. Because of their improved and cheaper creation, mostly a-Si cells in the sun were usually used for electronic devices with little or no power requirements, such as watches and pocket-sized various calculators etc.

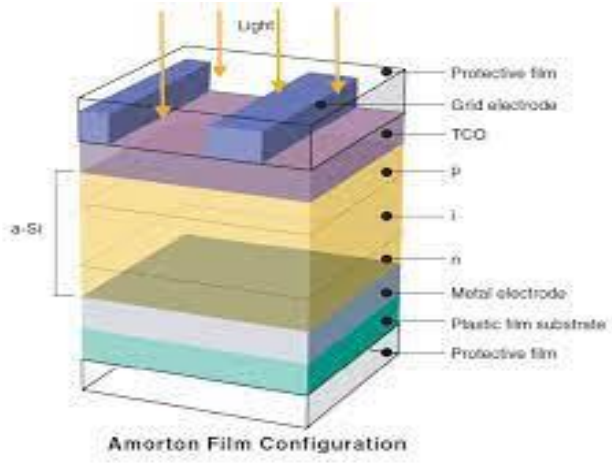

Figure 5:Basic structure of a-Si cells [8]

1.7 Thesis Scope

Regarding the problem of shading, which has a serious decline in the display of electrical phenomenon modules facing the sun at home, the accompanying pages show shadows that alter the energy and power yield in the sun of mainly photovoltaic panels. On the one hand, the opening part of the postulate contains on Associate in Nursing an instructive examine the functions of a solar supercharged charger. a short while later, a review of 2 chargers based mostly on daylight was calculated as soon as the shadows lie on them. The primary is calculable in the extraordinary center, wherever some circumstances are theoretically area units, as well as lighting or temperature, wherever 2 of them are considered, as it may not affect the operating results of the PV modules. However, another module examined was extremely calculable wherever weather patterns affected the results of devices in the module. In the course of the second part of the event, he again focuses on the presentation of 3 characteristic photovoltaic frames in the HiG center. The primary contains one electrical converter in an extraordinary array of six modules, another contains DC attention for each module and also the third frame contains a miniature electrical converter for every 2 modules in the same connection, having a complete of three miniature inverters and six modules. The gadget area unit additionally takes care to make sense in the following sections which will be discuss later in this research.

CHAPTER 2: LITREATURE REVIEW

2.1 Background

In order to better understand the topic and proposal, the research of this point has been directed to function as a basis for the dynamics in the postulation report and furthermore to take into account the framework of photovoltaics worldwide and at a more modest level. The energy result of the photovoltaic framework is affected by many external factors, for example, temperature, dust, concealment, sunlight-based light and sun-oriented frequency point and so on. Focusing on the exhibition of PV frames, Saint-Drenan et.al to decide on the main component that will affect the resulting age of a PV frame. It was also seen that four such limits - slope, point azimuth of PV modules, overall frame efficiency and imposed limit. Likewise, cloaking affects the outcome of the PV framework, but not much research has been completed on it yet.

The four boundaries referred to above add to the ability of a photovoltaic framework when suitable light is free, yet would decisively affect the results obtained when the modules are affected by hidden circumstances. Due to the evolution of the sun during the day and throughout the year, hiding occurs and cannot be deflected by any object located near the structure on which the PV panels are placed. The reduction in current and voltage limits created by the solar powered charger is evident under the cloaking effect [9].

A significant degree of energy mishaps and energy yield can be seen on the photovoltaic structure in a state of secrecy. In addition to the shadow that could be produced by nearby structures, objects, trees, or overhead fog, particles in the air would also affect the irradiance that the photovoltaic structure would receive. Unique radiation estimation tools are used to obtain the actual solar radiation hitting the Earth to account for environmental factors. The accuracy of the information would depend on the degree of time span for which the information was recorded. The Public Renewable Energy Research Facility is one of a pair where this information is continuously reviewed and collected. However, there are not many of these areas.

The ongoing research proposes a brief presentation on the numerous standards and properties of semiconductors and the electrical phenomena of solar powered cells. This includes a brief description of the CIGS leading edge of very thin film solar powered cells. The thesis primarily focused on the use of solar cells; therefore, the measurement of the basic estimate, a guide for the hypothesis and control of numerical and actual processes, is paramount. Since there are several

cycles in solar-oriented cells, our spoken communication is limited to the fundamental thickness of current versus voltage (I-V), Quantum potential, Eta (efficiency (just below brightness, η)) [10].

2.2 Basics of Solar Cells

Semiconductor materials have electrical properties somewhere in the middle between those of the conveyors in the case. They are neither good conductors nor good insulator, hence they are named semiconductors. It's a bunch of solids wherever there is a slight hole of a handful of volts within the spread of allowed energy states. According to the energy band hypothesis at T = 0 K, in a pure semiconductor material, this hole isolates one completely crowded band known as the valence band from one that is completely empty known as the conduction band. In order, as the temperature climbs as an example for T > 0 K, a limited number of electrons gain energy and move into the conduction band (free electrons) leaving states for electrons in the valence band (free holes). These free states (electron and holes) will gain motive energy from the half-life of the series states of the area units accessible to them on an individual basis, later they will respond to electric fields and focus slopes that take into account the naturally visible flow current. Figure 2.1 shows an examination of the defined band for 3 states of materials.

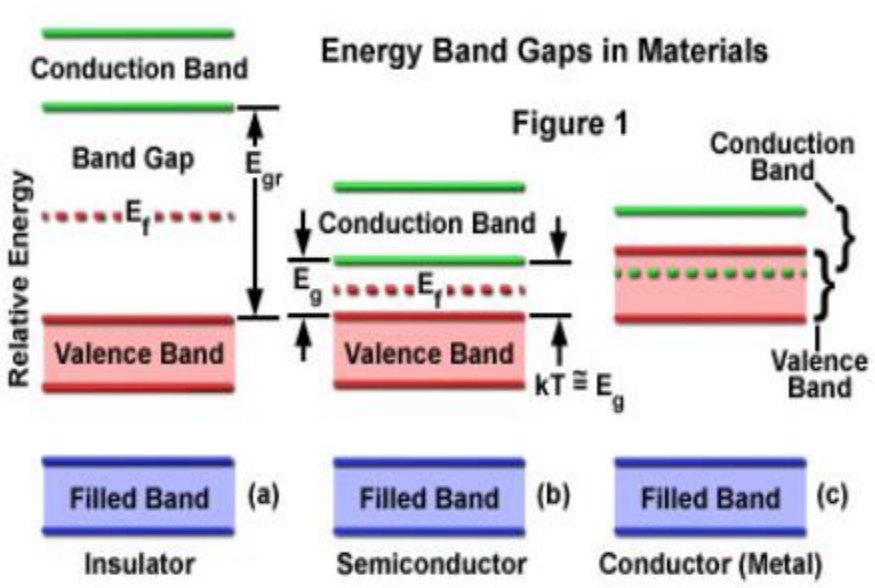

Figure 6:A detail of different bands in solids[10]

The main effective technique for deciding on the correct operation of a PV module is to quantify the complete I-V attributes. PV module datasheets provided by manufacturers contain math qualities for 3 places I, still in air under normal conditions. They also show the trademark I-V

bends for selected high-power solar irradiance tops and the PV module temperature. we tend to recognize 3 main components within the I-V intentional joint trademark which is show in below figure 2.2.

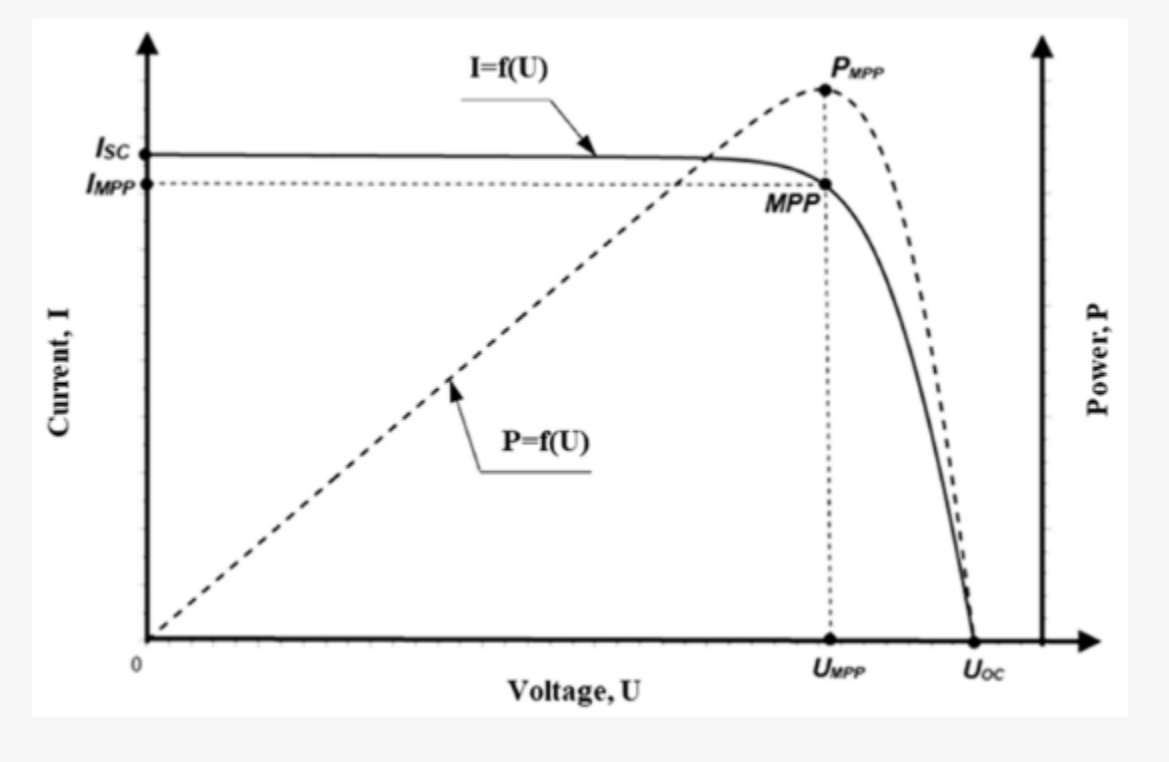

Figure 7:Current and Voltage graph in PV cells [10].

In states of steady and, oddly, primary-based solar radiation, the precisely calculable I-V curve is characterized by a neat shape and its monotonic reduction with increasing voltage and almost no apparent deviations or discontinuities. The status of the I-V mark depends on the standard and innovation of the cells making up the PV module. Because of the thin foil modules, especially the elemental modules, the bending is usually very accommodating in contrast to the bending of modules made of glass-like cells. The estimation of the I-V mark must be performed at a radiated power of not less than 700 W/m2 (as usual according to IEC/PN-EN 60891), which takes into account a number of specific changes in electrical limits obtained from bending at STC evaluated conditions. The direction of incidence of the rays is vitally important, which is initially controlled by a mechanical inclinometer. Deviations from the state of the standard trademark I-V shown in the image of the 2.2 areal units of peculiarities which potential variations of the areal unit shown in the image of the 2.3. completely different potential functions behind the deviations of I-V

qualities were bad within the article that were separated by screws from one to six in the image of the 2.3. The state of the I-V bend represented by the quantity one in figure 2.3 shows the errors in the range of current generated between the numerous areas of the PV module. The characteristic form of the step is that the impact of the bypass diode will shift the area under the control of the lower current. This gift circumstance occurs in several cases:

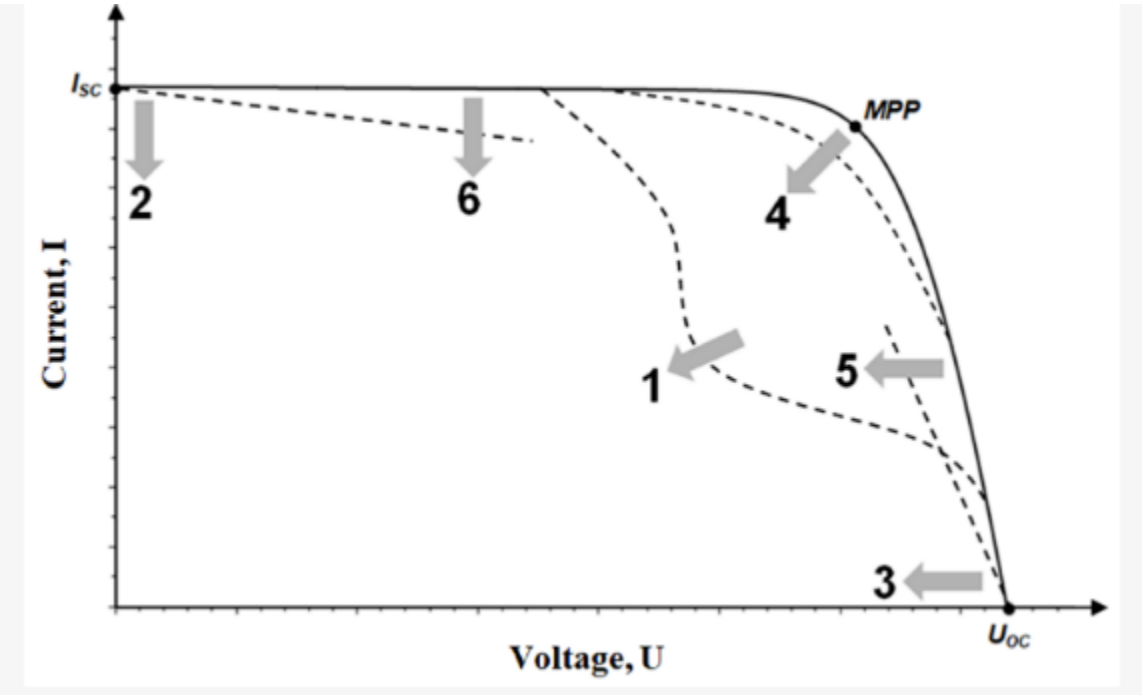

Figure 8:Deformation Current and voltage in PV cells [10].

2.3 Concept of single and double diode in PV Panels

2.3.1 Concept of single diode

The high growth of interest and thus the power of the electric phenomenon required accurate models of PV implementation. The definitive board model goes in an extended way within the truth of the conjecture about all the execution model PV range. The qualities of the PV module are approximated by the one-diode model (ODM), the two-diode model (TDM) with an additional diode, or the one-diode primary-based four-parameter model (OFPM) non-hereditary by discarding the shunt opposition.

[10] associated degree [11] introduced a recalculation for the method of 5 fuzzy ODM boundaries, which assumes the value of the diode quality problem. The results are exceptionally dependent on the diode value chosen, but a quality issue. In [12], it is planned to assess the properties under

conditions different from the qualitative conditions and then deal with the arrangement of nonlinear conditions at a similar time. This can be difficult and somewhat imprecise due to the nature of the temperature coefficients. Also, as framed in [13], simply interpreting the boundaries to a different temperature does not provide additional free terms. [14] determined ODM boundaries using a perplexed arrangement of model conditions using the filler part of number of attributes. This relies on an associate degree of experimental

connection for the padding part of the associated optimal cell stage. [15] introduced ODM boundary extraction by seeking and meeting equal unequal conditions. [15] to set model boundaries through a cerebral soft organization approach, which is extremely confusing and not exceptionally accurate. The extramural fit methods of [14] and [11] require real estimates, which are not particularly useful.

To reduce the frame requirement, [9] [10] and [11] planned to ignore the shunt obstacle and huge, submissions regarding OFPM. This allows logical bounds to be estimated, however at the expense of a loss of precision. In addition, boundary extraction for TDM is later completed with many unraveling and several flaws of speculation.

[12] expected the sinking currents of the 2 diodes to be equivalent, while [13] set qualities for the quality of the diodes factor. The technique for [14] needed semi-logarithmic graphs of commutable modulo, which are huge and not available.

In this work, a calculation is made to arrive at a decision on four ODM boundaries without much improvement or assumptions, depending only on the manufacturer's data sheets. The following received from TDM and OFPM are then contrasted with the trademark bend stated by the manufacturer in the data sheet. Error is then evaluated by drawing the root mean square error for 2 models. For circuit voltage and immersion current ODM for non-standard natural conditions is decided very accurately. In this research there are 2 models in a short time due to their comparable circuit contours.

2.3.2 Concept of double diode

There are many efforts to reduce the amount unclear boundaries and thus the process time for two diode model. while the desire to write, that is apparently saw most research coordinated with the

single-diode model [16], which can be attributed to its simplicity and less variety of fuzzy boundaries, making it much easier to look at and separate fuzzy boundaries from.

On the other hand, it is also okay to see that the single diode model is experiencing a fault that was once granted to the conditions of the evolving climate, which made it impossible to manage life. Consequently, the 2-diode model presents itself as a plausible explanation for the problem of climate selection impacts. However, the large variety of fuzzy boundaries and thus the process time prevent this model from being commonly used, as opposed to the 1-diode model. On the other hand, the noticeable accuracy achieved by this model contrasted, therefore, the single diode model; it is worth trying the experts to deal with the problems documented earlier.

Figure of both single and double diode model is mention in chapter 1 and discuss in detail over there.

2.4 Effect of shading on PV cells

A strategy is outlined to systematically assess the impact of shading on chargers based primarily on daylight and to estimate systematically despite the use of force-enhancing means. Completely different hidden things, for example, light, medium, and heavy quadratic measure thought out to find out what amount of yearly mishaps occur on a non-public PV system upwards. A consideration question is used which compares the prospects chances of probabilities of their occurrence as light overshadowing - the most extreme prospects and severe overshadowing - the least likely. On completely different PV frames that measure they are placed on the edge of each other and a direct created using open polyester texture with a thirty-seventh transport is completed. The framework wherever the tool was introduced had higher levels of creation, which is reflected in the results [17]. It likewise needs to be discovered that as subtle radiating shadow styles, its changeable nature that depends on district and also time will kick in, although this kind of strategy may not be completely affordable - direct concealment can provide another excellent examination management.

To mitigate the impact of the occlusion, the bypass diodes measured the square dimensions remembered for the PV institution. Square measure diodes associated with cells that square measure associated asynchronously. The diode square measurement converses unilaterally and the current can also cycle through all the cells that square measure the production once there is no shadow. in the case of a shadow on one of the cells, the diode of this cell can start directionally. in

this way, the continuation does not go through the hidden cell and also lightens the hiding result. Which is shown in below figure

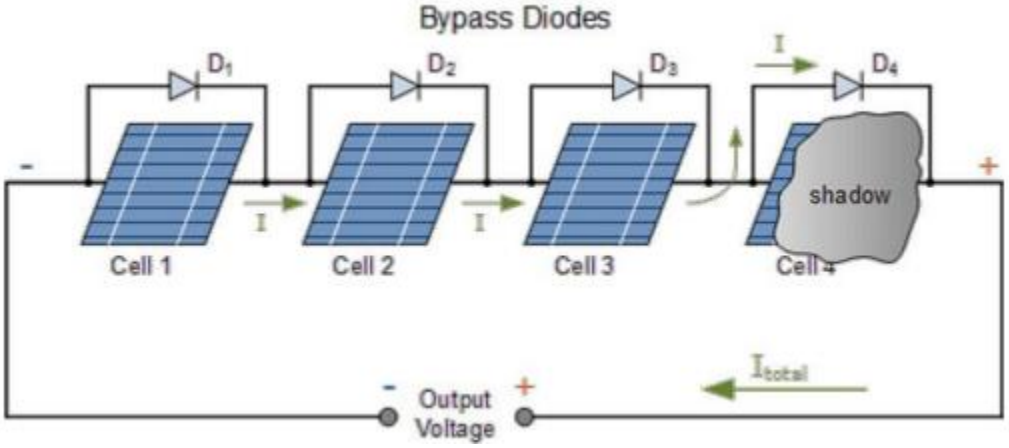

Figure 9:Connection of silicon cells with bypass diodes connected in series [17]

CHAPTER 3:

Modelling of Single and Double Diode

Mathematical representation of electrical phenomena primarily based on solar cells could be an important technique to check the quality of the planned current. This section presents the idea of a mathematical replica and its modelling of many actual models for, at intervals, physical peculiarities such as holes, recombination, and transport of charge carriers (holes and electrons) in materials of electrical phenomena. This can be completed with basic data boundaries to achieve predictable and satisfactory results. Having a typical gauge or start is an extremely useful purpose. This mathematical investigation can yield results for, matching demonstration outputs to search results, anticipating the impact of changes in material properties and calculating cell execution, and testing the utility of planned actual elucidation. Subsequently, sets of reference boundaries are presented that depict completely different (CdTe, CIGS, then beyond) flimsy solar-powered film cells. These models are used as typical for added complex models.

Explicit variants of electric phenomena (PV) cell innovations are used for various business activities. These cell improvements are delegated more clear, mono-glass and fine film. One- and two-diode photovoltaic models are widely used to display the traditional result for a photovoltaic module. The single diode model is the least problematic because it has an ongoing AN supply in series with the diode. This model is updated to include 1 series of obstacles. Regardless of its ease, it shows the intense shortcomings of the once-old temperature variations. A model growth that represents a useful opposition to the shunt R_P shown in Figure 3.1. Although major progress is being made, this approach requires major registration efforts. moreover, its accuracy decreases in low irradiance, especially near the electrical circuit voltage (V_{oc}). The two-diode model (containing R_P and R_s) shown in Figure 3.2 is usually recommended for greater accuracy [18].

3.1 Modelling of single diode

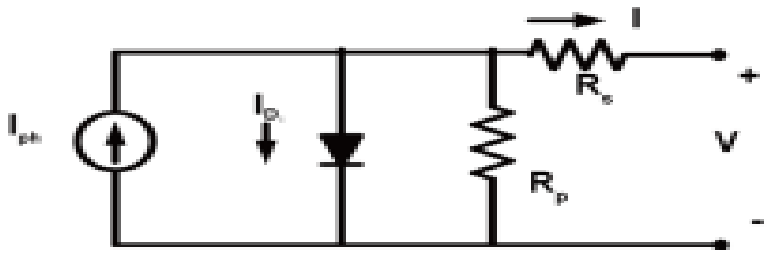

Figure 10: Single diode model of PV cells and its Electrical model [18].

The equation for current in single diode model will be as follows:

$$I = I_{ph} - I_o \left[\exp\left(\frac{V + IR_S}{aV_T}\right) - 1\right] - \frac{V + IR_S}{R_p}$$

In the above equation the following terminologies representations are:

When light suddenly falls on the surface of PV cells which create current that type of current is represented by I_{ph} which is show in the above equation. The output current of the PV cells is represented by I_o. I is the current of the PV cells and V is the voltage of PV cells. Thermal voltage of the PV cells is represented by V_T. R_S and R_p is the resistance of PV cells in single electrical diode model which is show in figure 3.1. And a is ideal for single diode model.

Now the equation for thermal voltage is:

$$V_T = \frac{N_s KT}{q}$$

In the above equation of thermal voltage K is the Boltzmann constant and its value is fix that is [$1.3806503 \times 10^{-23}\, j/k$]. T stands for temperature, N_s represents number of diodes connected in series. And q represents the charge of electrons again its value is constant which is [$1.60217646 \times 10^{19} c$].

Now we will the equation for I_{ph}:

$$I_{ph} = \frac{G}{G_n}[I_{pvn} + K_1(T - T_n)]$$

Now equation for the output current I_o will be as follows:

$$I_o = I_{on}\left(\frac{T_n}{T}\right)^3 \exp[\frac{qE_g}{ak}(\frac{1}{T_n} - \frac{1}{T})]$$

And last equation is for current due to diffusion is:

$$I_{on} = \frac{I_{scn}}{\exp\left(\frac{V_{ocn}}{aV_{Tn}}\right) - 1}$$

3.2 Modelling of Double diode

In the double modeling of diode, the only difference as on can compare it with single diode is that in this model one extra diode is connected in parallel rest of the phenomena remain the same.

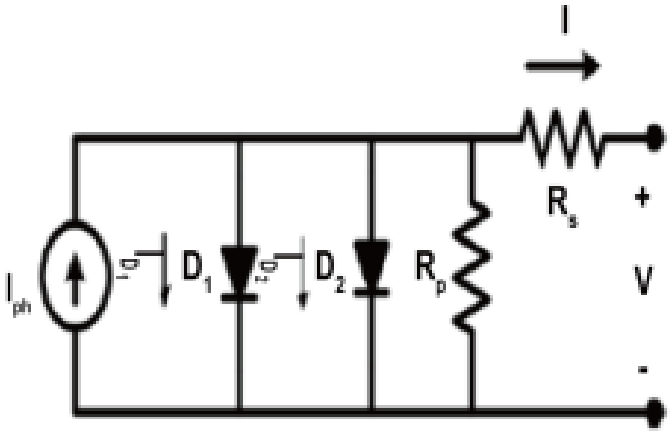

Figure 11: Double diode model of PV cells and its Electrical model [18]

The different equations for double diode model will be as follows:

Equation for overall current is:

$$I = I_{ph} - I_{d1} - I_{d2}$$

Here in the above equation the total current is the difference between the current produce due to light source and the current which is generated in both the diode I_{d1} and I_{d2} respectively.

Now equation for the current in I_{d1} will be as follows:

$$I_{d1} = I_{o1}\left[\exp\left(\frac{V + IR_s}{a_1 \times V_t}\right) - 1\right]$$

In the above equation I_{o1} is the saturated current of first diode which is D_1.

Now equation for second diode current will be as follows:

$$I_{d2} = I_{o2}\left[\exp\left(\frac{V + IR_s}{a_1 \times V_t}\right) - 1\right]$$

Now if we put the current values of first diode and second diode in the top most equation the total current will become as follows:

$$I = I_{ph} - I_{o1}\left[\exp\left(\frac{V + IR_s}{a_1 \times V_t}\right) - 1\right] - I_{o2}\left[\exp\left(\frac{V + IR_s}{a_2 \times V_t}\right) - 1\right] - \frac{V + IR_S}{R_p}$$

Here in this double diode model the current generated due to fall of light on the surface of solar cell the equation will be as follows for that:

$$I_{ph} = \frac{G}{G_n}[I_{pvn} + K_1\Delta T]$$

In the above equation G_n is the irradiance.

Now the saturated current which is in reverse bias for both the diodes the equation will be as follows for that:

$$I_{o1} = I_{o2} = \frac{I_{scn} + K_1\Delta T}{\exp\left(\frac{V_{ocn} + K_V\Delta T}{(a_1 + a_2)/p \times V_T}\right) - 1}$$

The above equations which is mention in topic 3.1 and 3.2 are equations for single and double diode modelling.

3.3 Efficiency of the diode model

The range of output energy of a solar cell for the energy input from the solar is defined as expertise. While they reflect the capabilities of the solar cell itself, productivity depends on the variability and strength of daylight incidence and thus the temperature of the solar cell towards solar panels. Thus, the conditions that the square measure used to quantify effectiveness should be carefully controlled to connect the exhibit of 1 device to another. The main structure problem is indicated because the ratio of the best energy yield from a primarily daylight-based cell to the circuit voltage and termination in results [19].

Now for efficiency of the diode model we will write the equations the first equation is the form factor which is represented by FF:

$$FF = \frac{V_m I_m}{V_{oc} I_{sc}}$$

In the above equation V_{oc} is the voltage in case of open circuit and I_{sc} is the current in case of short circuit.

For finding the efficiency the equation will be:

$$\eta = \frac{V_{oc} I_{sc} FF}{P_{in}}$$

In the above equation P_{in} is the input power.

Now the equation for change in temperature will be:

$$\Delta T = T - T_n$$

In the above equation ΔT is the change in temperature , T is the specific temperature , and T_n is the standard temperature for all testing conditions.

3.4 Observed values during Simulation

To explore the behavior of each PV model, a recreation is worked in MATLAB simulation. The same data are used to distinguish the PV models and to investigate the effect of different boundaries. These determinations are summarized in Table 1

Table 1: Values and specification of PV cell is listed below

Reference Temperatures	15°C ,25 °C, 45°C
Input Power	99 W
Short circuit current	8.67 A
Open Circuit Voltage	37.92V
Temperature coefficient of open circuit voltage	-0.33%°C
Temperature coefficient of short circuit current	0.06% °C

3.5 Irradiance

The efficiency of a photovoltaic device depends on the spiritual scattering of solar radiation. The sun can be a source of sunlight and its radiation can change with the variability of a natural object at the 6000 K point. Electromagnetic radiation of all the frequencies listed is maintained and produced by a dark body.

Investigating the impact of solar radiation on photovoltaic devices is difficult due to the fact that daylight fluctuations on the outside of the Earth are compact components, such as temperature variability on the sun mainly based plate and thus the result of inclusion [20].

3.6: PROBLEM STATEMENT AND METHODOLOGY

3.6.1 Basic Parameters

A hypothetical examination of the electrical phenomenon mechanism visible from the recreations is used to induce a perfect arrangement of boundaries for the planned model. Thus, the mathematical representation of crystalline slender foil cells powered by solar vapor can be an important procedure to check the feasibility of planned real-world clarifications and to predict the effects of real-world changes on cell performance. For this work, the correct data about the attached field is significant for modulating new problems even on a secured person and further developing presence models. Procedures that need to be taken into account while entry boundaries for mathematical models are currently being explored here, in addition express reference boundaries for PV gadgets (CIGS, CIS, a-SI and CdTe) are planned this way. All of the trials discovered within the procedure associated with CIGS and alternative usual cases have terribly close to the typical initial stage, even though the computations in the different scenario were performed at different stages and lightweight from different viewpoints. a number of faculties and associations for alternative innovative work, such as Colorado State University, University of South Wales and Ghent University, are trying to support models visible by mathematical demonstration on materials for a representative thin film process based mainly on solar cells. Since the 1980s, various models for configuration functions have been created and used. The lack of a concrete model suggests more efforts to make sense of the confusing construction of poly glass-like materials. Efforts are made to find an explicit receptive articulation for the J-V trademark. The

reproductions, if accurately used and accurately deciphered, will be excellent compliments for rehearsals and provide excellent data on how to behave in elegant film equipment [21].

3.6.2 Problem Statement

Physical and chemical properties of solar cell material and model influence the susceptibility of PV against shadowing. Identification of factors which impact output voltage, current and power is required for establishing set of protocols for recommendation of PV materials for specific load demand and weather conditions.

The main objective of this research is:

- To investigate the behavior of different PV materials under different shading conditions.
- To identify different factors which affects output of specific PV materials.
- To establish set of recommendations for the adoption of different PV materials for specific environmental conditions.

3.6.3 Proposed Methodology

In this proposed methodology the first step is that we have to established 6×6 PV system, after establishing 6×6 PV system then we select the materials which in our case is CIS. CdTe, CIGS, a-SI. After this we have to select the diode model in this research we select two types of diode model that is single diode model and double diode model. After this we will calculate current and voltage and PV curve at standard temperature. Next step is to establishing the shading pattern and show different impacts of temperature on that patterns. And then we have to calculate the current voltage and PV curve at Non STC conditions and last step is to analyze and comparison between both STC and Non STC conditions. The overflow is given in the below figure.

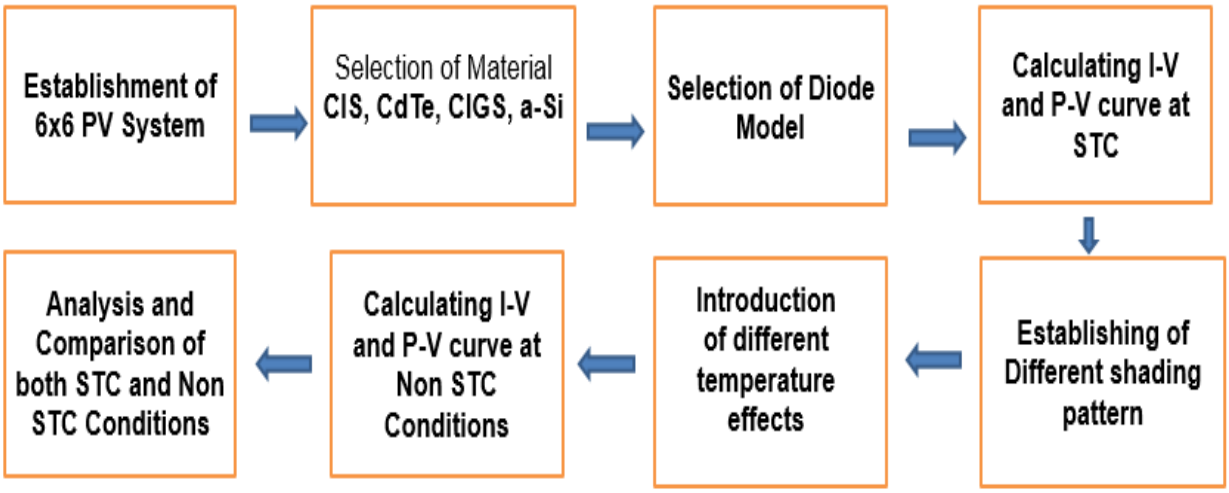

Figure 12: Research Flow

3.7 Schematic Diagram

The below figure is schematic circuit diagram of 6x6 model.

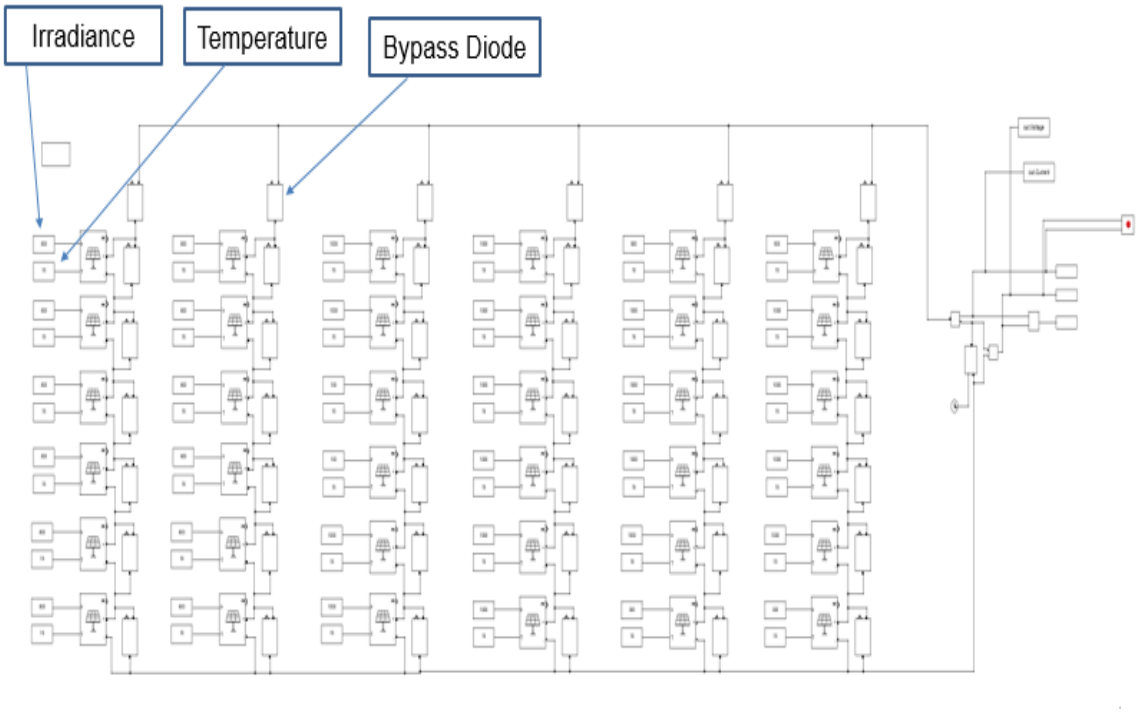

Figure 13: schematic circuit diagram of 6x6 model

3.8 Shading Patterns

In the below figure different shading has been shown and each shading mark different color which has different values as shown below. These are the four shading pattern. We have made I-V and P-V curve based on these four shading patterns. As we have already said that there are 4 different materials which are experimented on three different temperature effects and four different shading pattern. We have use a Matlab to make I-V and P-V curve. We have selected each material one by one for all the 36 modules for three different temperatures and plot I-V and P-V curve to see the behavior of curve and the maximum power of each material.

Figure 14: Four Shading Patterns

CHAPTER 4:

RESULTS AND DISCUSSION

In this chapter we will discuss and do analysis of the results which comes from our simulation. Our results are based on single and double diode and also we use four different materials and see its nature at different temperature using four different materials. All the results will discuss in below figures.

4.1 Results and discussion based on single diode model

In the below figure we have already said that there are 4 different materials which are experimented on three different temperature effects and four different shading pattern. But let see the effect of all materials without shading. At the bottom right we can see 6x6 system with irradiance level of 1000w/m^2. And three different graph at temperature 15,25 and 45 degrees The first graph which is against 15 degrees we can see Short circuit current on Y axis and Open circuit voltage on X axis.

The CIS has the higher short circuit due to the presence of Zinc Oxide and Cadmium disulfide in its structure as they both have good optical properties and short circuit current depend upon the optical property which is the absorption and reflection of sunlight.

Whereas the amorphous silicon has higher open circuit voltage due to its higher band gap which is 1.78eV because Voc depend upon the band gap of a material higher the band gap higher will be the Voc. We can also see CIS and CIGS with the same Voc this is because they have same band gap of 1.2eV. While Cdte has optimal band gap which is 1.48eV.

Now let's see the temperature effect when we increase the temperature from 15 degrees to 25 C the Voc of all materials decreases similarly for 45 C the Voc further decreases the reason behind this is the Voc also depends on temperature as the temperature increase the band gap of materials decreases hence it decreases the Voc.

Analysis of different Solar Cells using various materials without Shading at different temperature

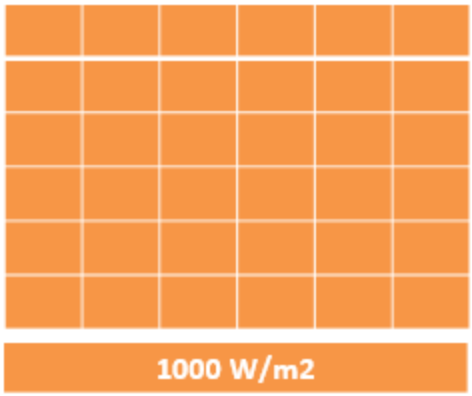

Figure 4.1 a: Pattern without shading

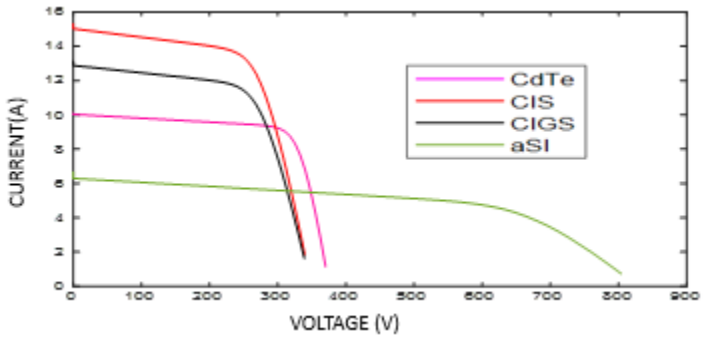

Figure 4.1 b: Current and Voltage graph at 15 ℃

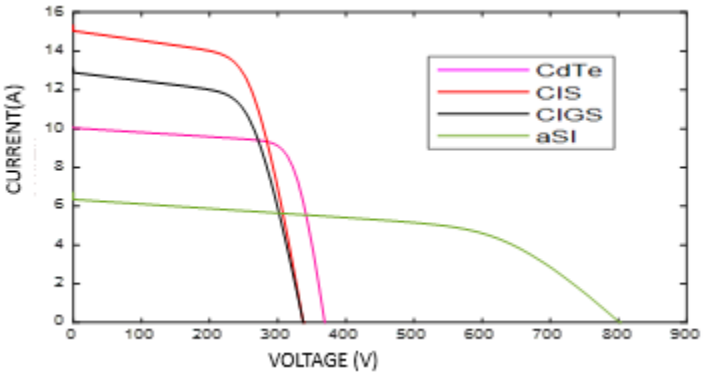

Figure 4.1 c:Current and Voltage graph at 25 ℃

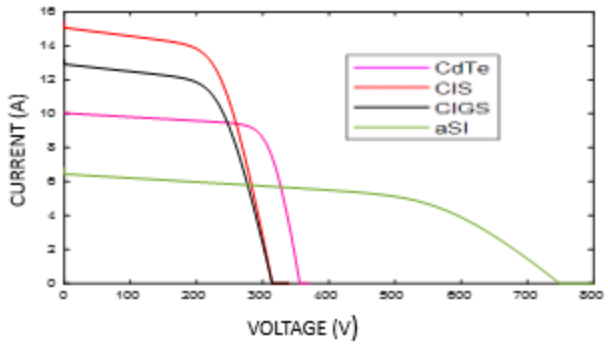

Figure 4.1 d:Current and Voltage graph at 45 ℃

In the figure 4.2 these are the P-V graphs with the same pattern without any shading. We can see the maximum power in the boxes. And this is our main aim to check the effect on maximum power of all materials after applying shading but in this case there is no shading we will see the shading in upcoming slides.

But If we see the first graph where temperature is 15 we can see the Maximum Power of a-si is 2853W but upon increasing the temperature up to 25 and 45 the power has reduced to 2770 W and 2595W. Because when the solar cells get hot the voltage reduce and therefore the power is also reducing.

P-V Analysis of different Solar Cells using various materials without Shading at different temperature.

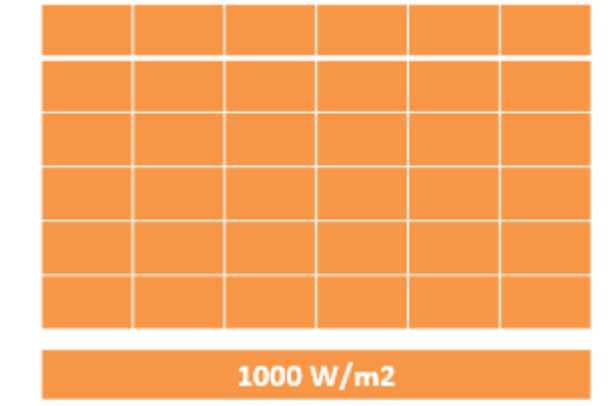

Figure 4.2 a: Pattern without shading

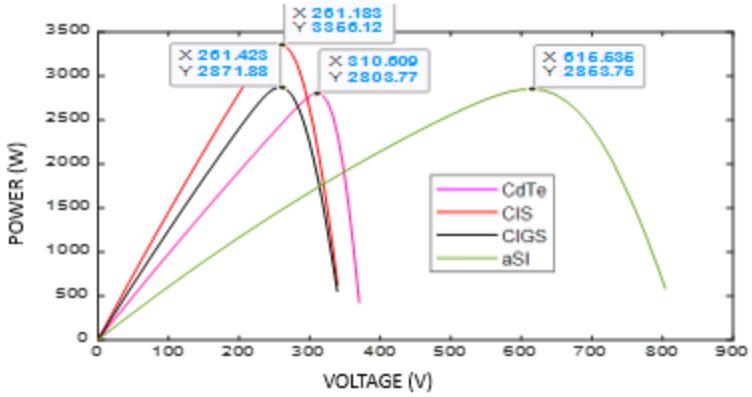

Figure 4.2 b: Power and Voltage graph at 15 ℃

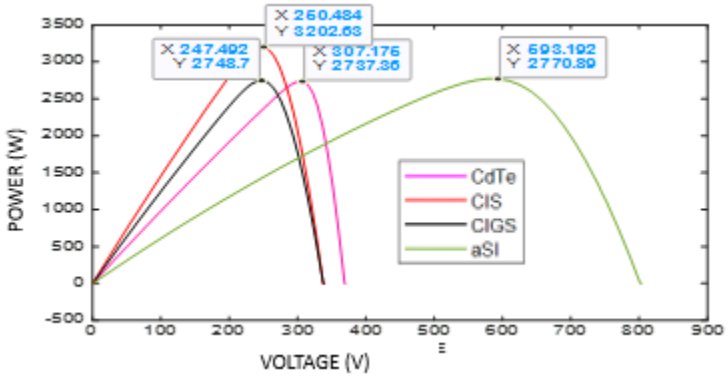

Figure 4.2 c:Power and Voltage graph at 25 ℃

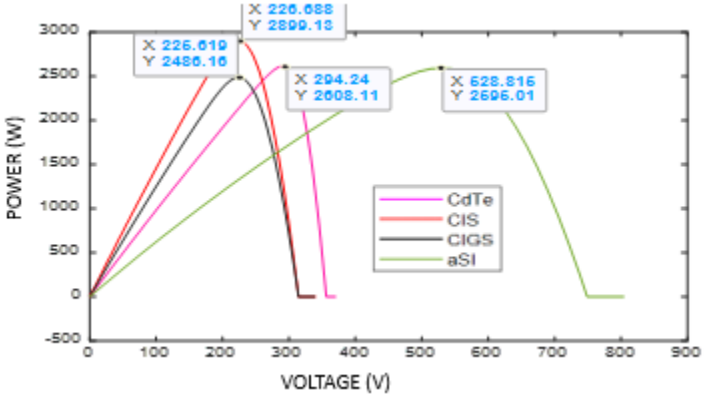

Figure 4.2 d:Power and Voltage graph at 45 ℃

.

In the figure 4.3 Now let see the effect when we have shading on different modules. This is the shading pattern 1. As we can see first two columns are shaded with 800W/m^2 represent the blue color.

As we can see the Short circuit current is reducing of all four materials this is because when shading comes on Parallels modules the current pass through the unshaded modules and neglect the path of shaded region.

So in this case 4 strings are unshaded so short circuit current of all material has reduced for example the Isc of CIS was 15A but due to parallel shading it has reduced to 14A. In these 3 temperature effects the Voc is also reduce due to increase in temperature as already discussed.

Now I-V Analysis of different Solar Cells using various materials with Shading Pattern 1 at different temperature.

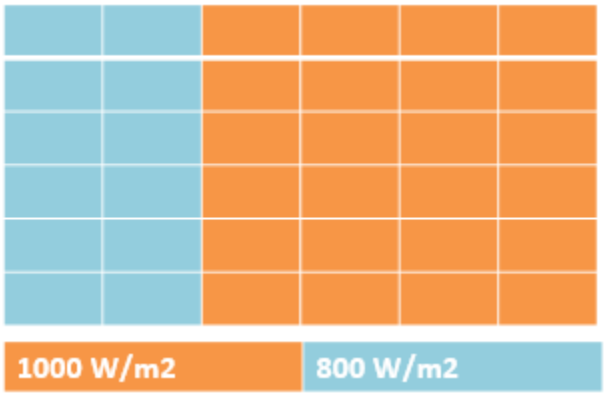

Figure 4.3 a: Pattern with shading

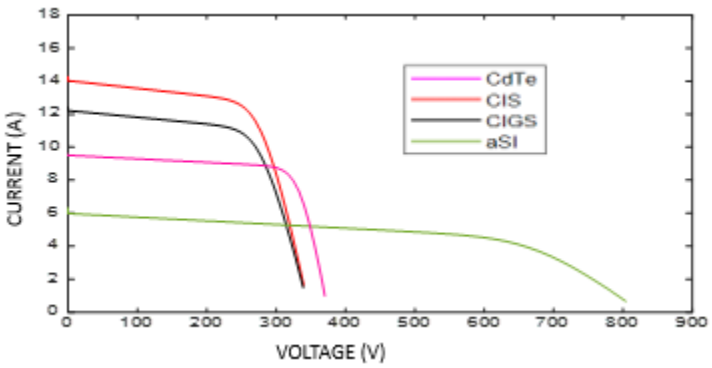

Figure 4.3 b:Current and Voltage graph at 15 ℃

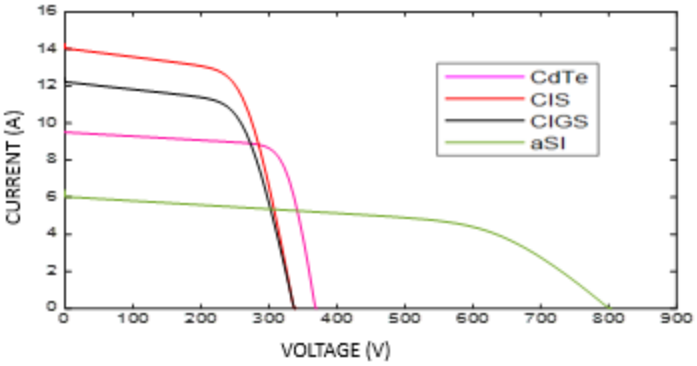

Figure 4.3 c:Current and Voltage graph at 25 ℃

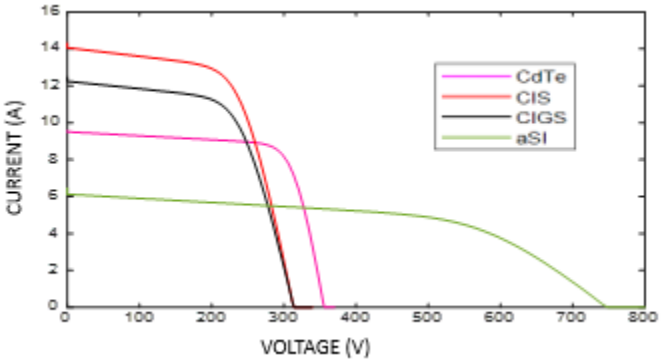

Figure 4.3 d:Current and Voltage graph at 45 ℃

Now in the figure 4.4 we will look to the PV curve of the same pattern. As both Short Circuit current and Open circuit voltage is reducing here due to the effect of shading and Temperature. The power in all three graphs are reduced. If we see the power without shading amorphous silicon at 15 C it was 2853W but after both shading and temperature effect it has reduced to 2722W which is 4.6% reduction in maximum power.

P-V Analysis of different Solar Cells using various materials with Shading Pattern 1 at different temperature.

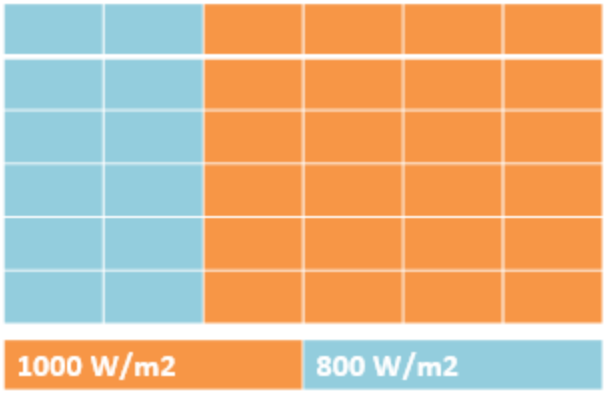

Figure 4.4 a:Pattern with shading

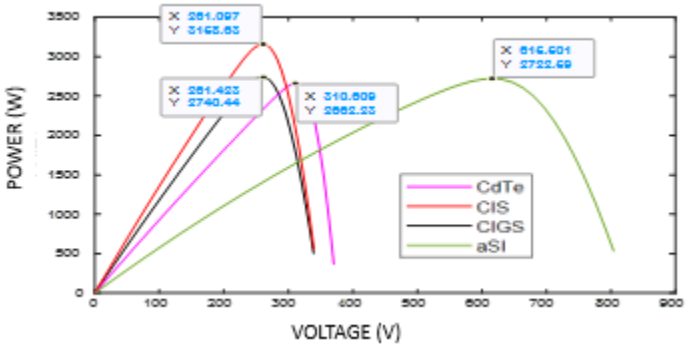

Figure 4.4 b:Power and Voltage graph at 15 ℃

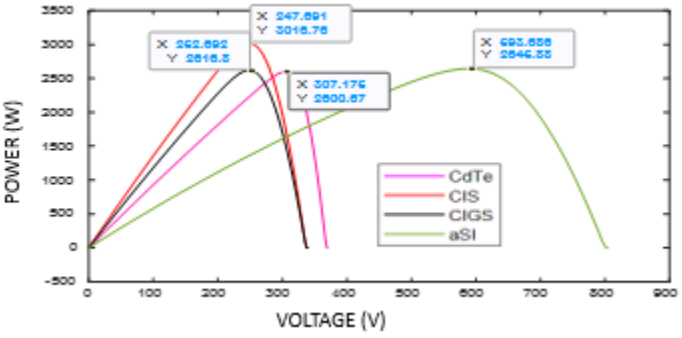

Figure 4.4 c:Power and Voltage graph at 25 ℃

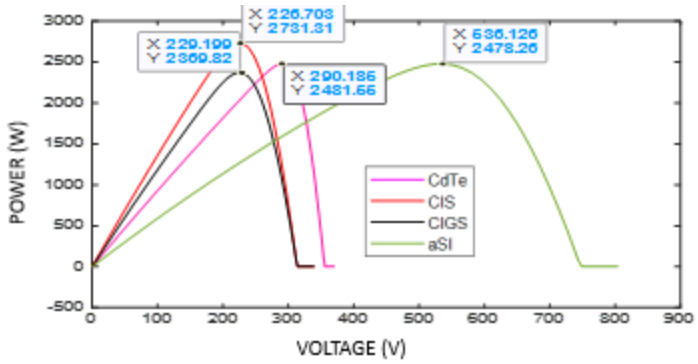

Figure 4.4 d:Power and Voltage graph at 45 ℃

Now in the figure 4.5 let's change the shading pattern. This time the last two rows are shaded with 800w/m2. The short circuit is 15A of CIS as it was previously 14A when shading came at parallel because now the current has flowing through all four strings. but we can see steps in the curves of 3 materials as when the shade comes on Series Module those modules make less current hence to avoid the flow of current backward we use reverse bias bypass diode so current can pass through these bypass diode which reflect the step in curves. But we can see a-SI which does not shows any steps in its curves this is because amorphous silicon has a non-crystalline shape and its absorption rate is also very high so it is good against shadowing by increasing the shadow it will shows less changes in its curves as compared to other 3 curves.

Now I-V Analysis of different Solar Cells using various materials with Shading Pattern 2 at different temperature.

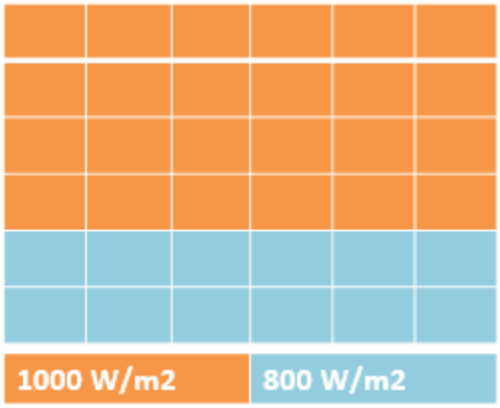

Figure 4.5 a:Pattern with shading

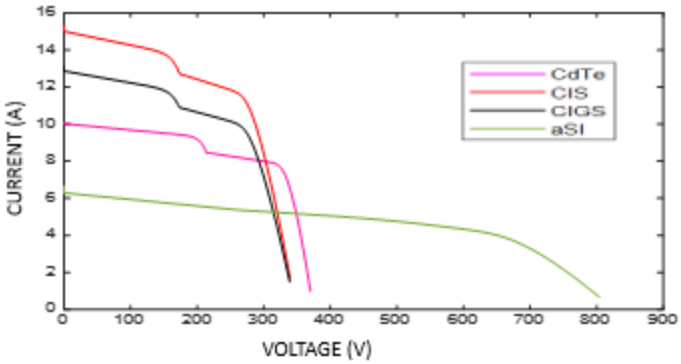

Figure 4.5 b:Current and Voltage graph at 15 ℃

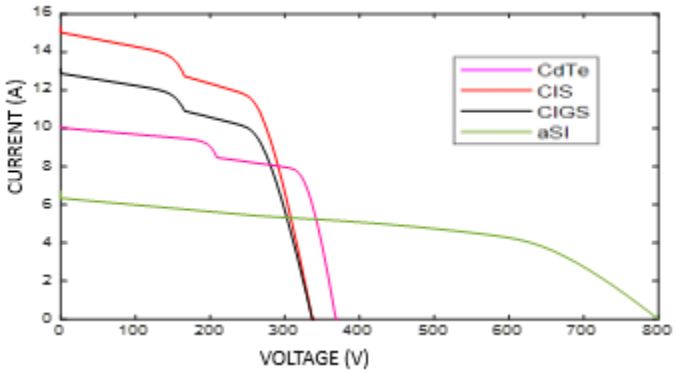

Figure 4.5 c:Current and Voltage graph at 25 ℃

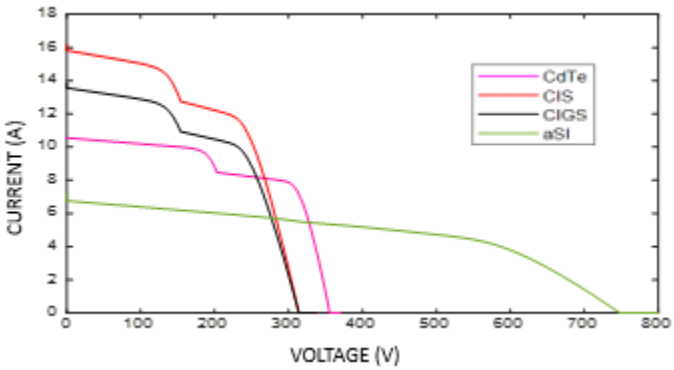

Figure 4.5 d:Current and Voltage graph at 45 ℃

Now in figure 4.6 we will do PV analysis for the same shading pattern we analyze the P-V Curve here. As we can see the steps in the power as well due to use of bypass diode as already discussed. And we can see the two peaks one is Global peak which has the maximum Power and the other is Local Peak. The power in this case is also reducing with the increasing in temperature. As it can be seen as increasing temperature from 15C to 25C the power of all four materials has reduced. In case if we the reduction in the power of a-SI after shading so we will see that 8% of the power has reduced

as compared to when there was no shading. So we can say that whenever a shading occurs at series it reduces the more power as compared to parallel shading.

P-V Analysis of different Solar Cells using various materials with Shading Pattern 2 at different temperature.

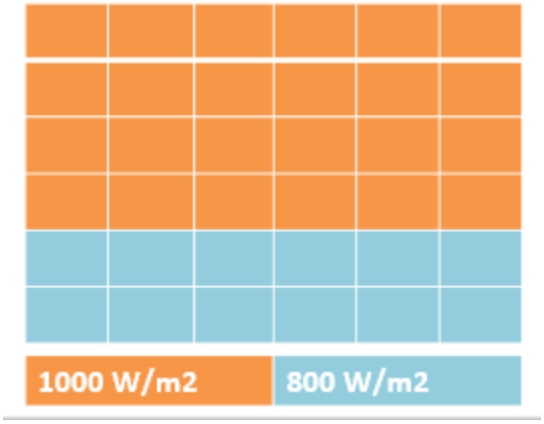

Figure 4.6 a: Pattern with shading

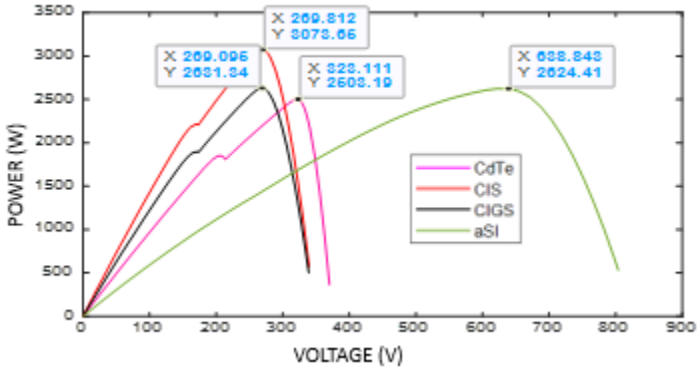

Figure 4.6 b:Power and Voltage graph at 15 ℃

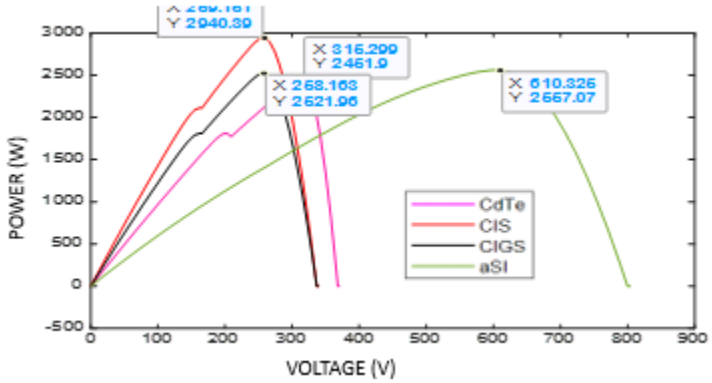

Figure 4.6 c:Power and Voltage graph at 25 ℃

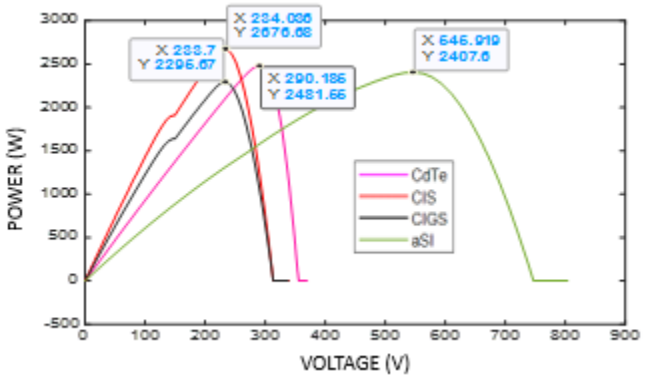

Figure 4.6 d:Power and Voltage graph at 45 ℃

Now in figure 4.7 we see the effect on I-V curve for non-uniform shading as shading is on different module and have different irradiance level. The short circuit current is reduced of all four materials as discussed previously due to first two string shading the last 4 strings are generating the current. And now the steps have also increase because we have placed shading on different module so whenever the current flow through the bypass diode and neglect the shaded modules the steps will appear in curves and this will increase when the shading increases. Now the increased shading has also start effecting a-SI but still the curve is smooth as compared to other due to its high absorption rate. And the other reason is that non crystalline shape material do not develop a hot spot region in the same manner as crystalline materials.

I-V Analysis of different Solar Cells using various materials with Shading Pattern 3 at different temperature.

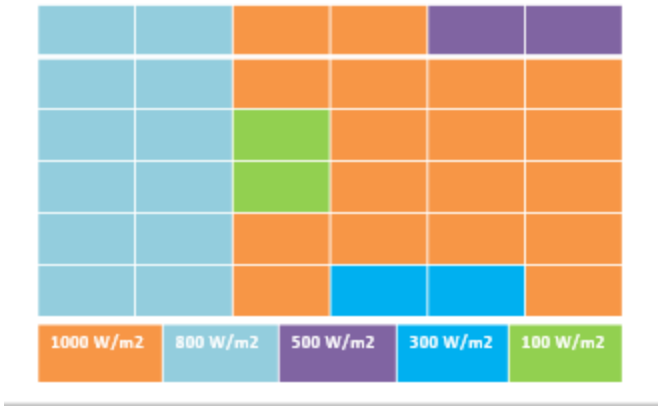

Figure 4.7 a:Pattern with shading

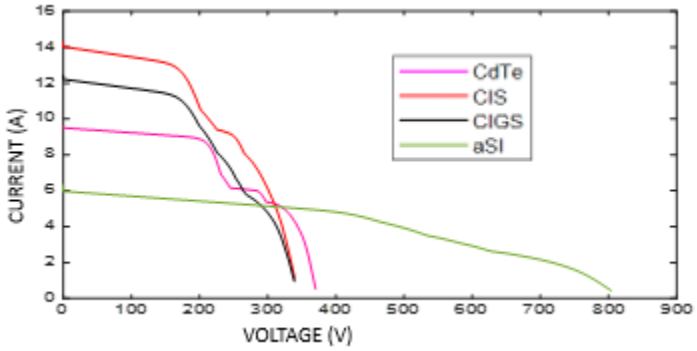

Figure 4.7 b:Current and Voltage graph at 15 ℃

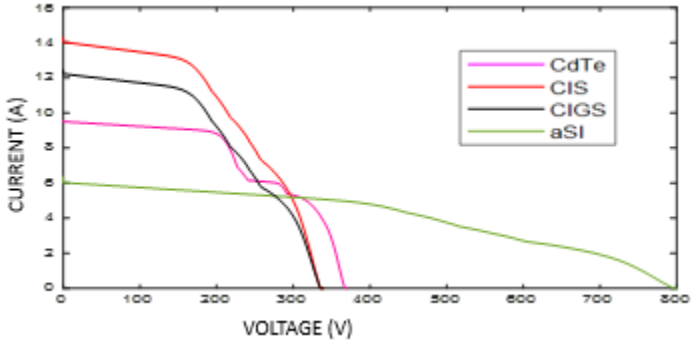

Figure 4.7 c:Current and Voltage graph at 25 ℃

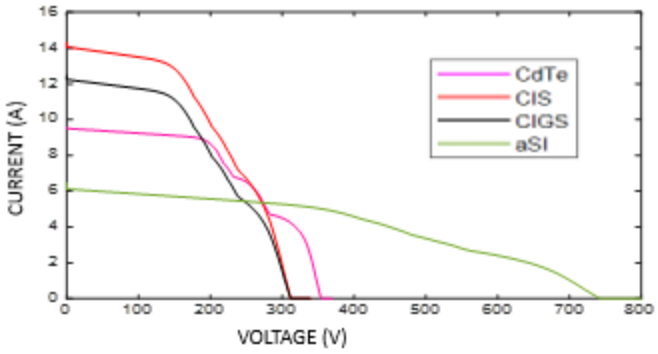

Figure 4.7 d:Current and Voltage graph at 45 ℃

Now in figure 4.8 we will see the effect of this shading pattern on P-V curve. Now we can see the increased local peaks in all three graphs due to the shading at different materials. Global peaks represent the maximum power while all other peaks are local peaks. So high shadow has also effect the smoothness of all curves in all three temperature effects. And the power of all materials has reduced to very low level if we compare the maximum power without shading and this specific shading pattern the power is reduced to 30% now. So this proves as the shadow increases the maximum power will further decreases.

P-V Analysis of different Solar Cells using various materials with Shading Pattern 3 at different temperature.

Figure 4.8 a:Pattern with shading

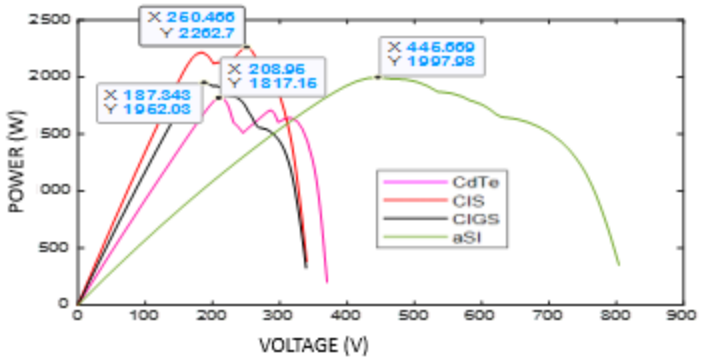

Figure 4.8 b:Power and Voltage graph at 15 ℃

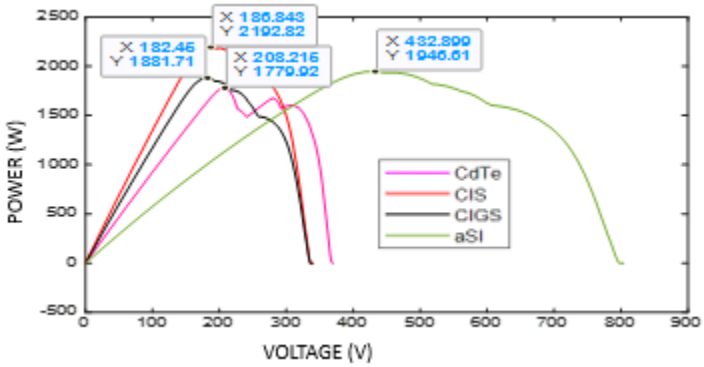

Figure 4.8 c:Power and Voltage graph at 25 ℃

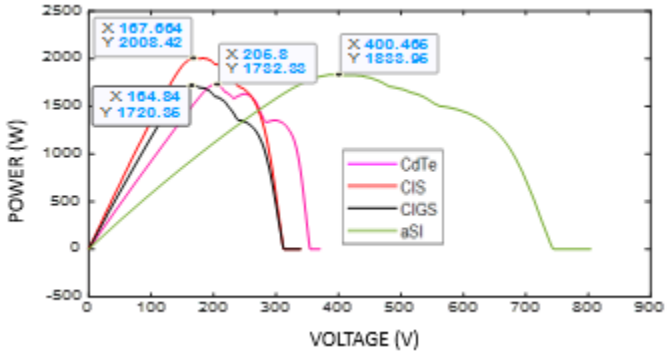

Figure 4.8 d:Power and Voltage graph at 45 ℃

Now in figure 4.9 we will see Final shading pattern which is also a non-uniform shading in this pattern shade is reduced and placed at different modules. The effect is same further increasing the shading will further effect the curve and steps will appear on all materials curves.

I-V Analysis of different Solar Cells using various materials with Shading Pattern 4 at different temperature.

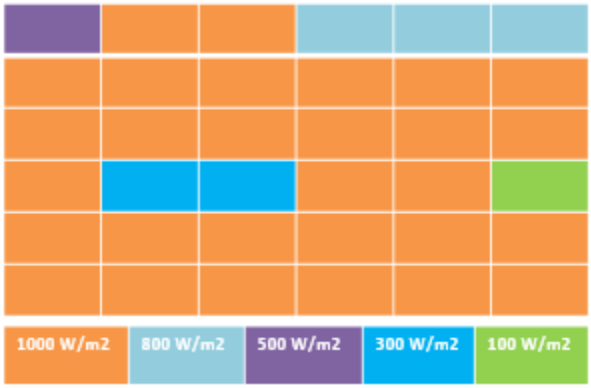

Figure 4.9 a: Pattern with shading

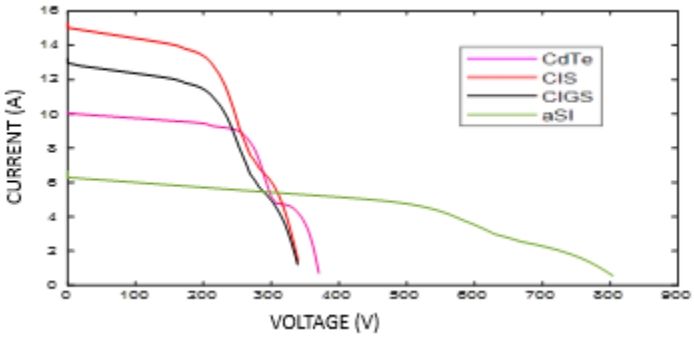

Figure 4.9 b:Current and Voltage graph at 15 ℃

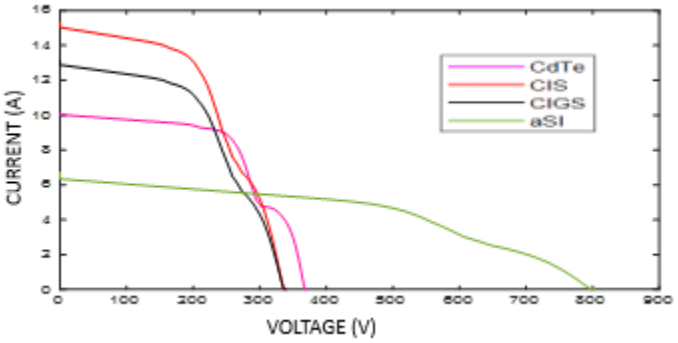

Figure 4.9 c:Current and Voltage graph at 25 ℃

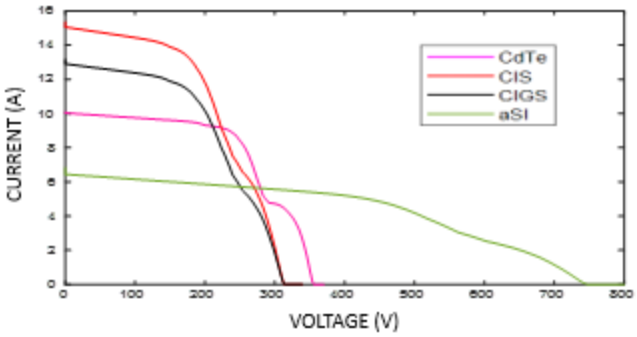

Figure 4.9 d:Current and Voltage graph at 45 ℃

Now in figure 4.10 we will see the global and local peaks here too due to the shading at different modules. Power has also reduced here with the effect of temperature and shading as it can be seen in the three graphs. Similarly, if we see the reduction in the maximum power here which is almost 15.8% reduction as compared to non-shading. These were the all the all four shading pattern and now have look at the combine results in table form.

P-V Analysis of different Solar Cells using various materials with Shading Pattern 4 at different temperature.

Figure 4.10 a:Pattern with shading

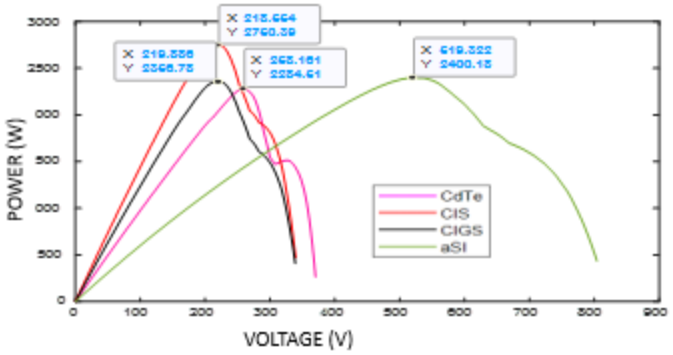

Figure 4.10 b:Power and Voltage graph at 15 ℃

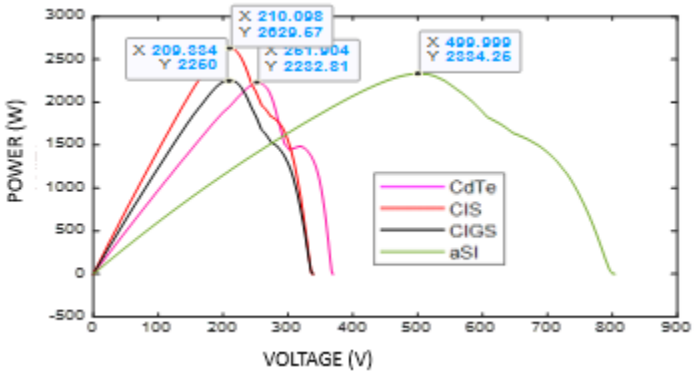

Figure 4.10 c:Power and Voltage graph at 25 ℃

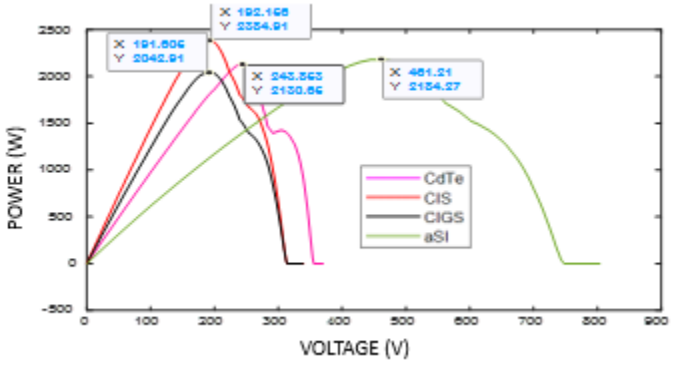

Figure 4.10 d:Power and Voltage graph at 45 ℃

Now in figure 4.11 we will see the table which I have made using the I-V and P-V curves shown in above slides for three different temperatures. The first two pattern we can see on a right side. Here it is the comparison of three different temperatures against same shading pattern. As we can see the amorphous silicon has the high Voc while CIS has the high short circuit current and maximum power due to its highest lab efficiency of 22.9%. It can be further seen that upon increasing temperature the VOC is decreasing. When comparing the above two table we can see the Short

circuit current is less in Pattern 1 due to shading at first two columns for pattern 1 at 15 degree of CIS it was 14 and for second pattern it is 15. The reason already shared that for first two column shading only last 4 strings are generating current.

OBSERVATION FROM I-V AND P-V DATA FOR PATTERN 1 AND 2.

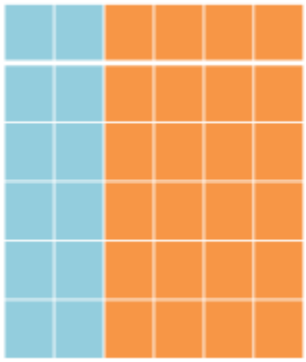

Figure 4.11 a: Pattern 1 With Shading

Values of Isc , Voc , Pmp at different conditions for shading pattern 1									
Material	15 °C			25 °C			45 °C		
	Voc(V)	Isc(A)	Pmp(W)	Voc(V)	Isc(A)	Pmp(W)	Voc(V)	Isc(A)	Pmp(W)
aSi	**805**	6.0	2722	**800**	6.0	2645	**750**	6.0	2478
CIS	350	**14**	**3158**	340	**14**	**3016**	320	**14**	**2731**
CIGS	350	12.2	2740	340	12.2	2616	320	12.2	2369
CdTe	370	9.7	2662	360	9.7	2600	350	9.7	2481

Figure 4.11 b:Values of Isc, Voc, Pmp at different conditions for shading pattern 1

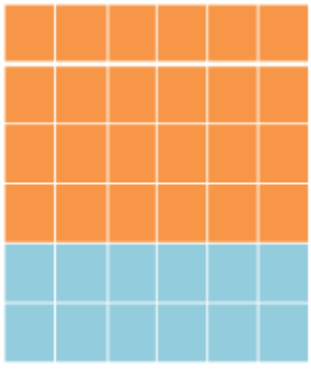

Figure 4.11 c:Pattern 2 with shading

Values of Isc , Voc , Pmp at different conditions for shading pattern 2									
Material	15 °C			25 °C			45 °C		
	Voc(V)	Isc(A)	Pmp(W)	Voc(V)	Isc(A)	Pmp(W)	Voc(V)	Isc(A)	Pmp(W)
aSi	**805**	6.3	2624	**800**	6.3	2557	**750**	6.3	2407
CIS	350	**15**	**3073**	340	**15**	**2940**	320	**15**	**2676**
CIGS	350	13	2631	340	13	2521	320	13	2295
CdTe	370	10	2503	360	10	2451	350	10	2441

Figure 4.11 d:Values of Isc, Voc, Pmp at different conditions for shading pattern 2

Now in figure 4.12 we will see shading pattern 3 & 4. As we can see the even with the high shading the CIS still giving the higher maximum power among all four materials. And but the power is reduced to around 2000W in shading pattern 3 due to high shading at pattern 3. So this prove the shadowing decrease the maximum power as the maximum power increases.

OBSERVATION FROM I-V AND P-V DATA FOR PATTERN 3 AND 4.

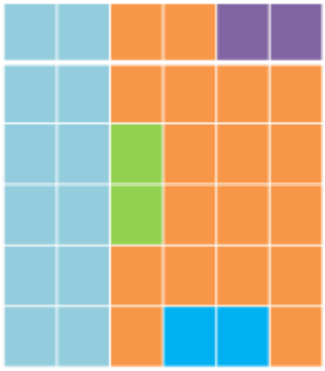

Figure 4.12 a:Pattern 3 with shading

Values of Isc , Voc , Pmp at different conditions for shading pattern 3									
Material	15 °C			25 °C			45 °C		
	Voc(V)	Isc(A)	Pmp(W)	Voc(V)	Isc(A)	Pmp(W)	Voc(V)	Isc(A)	Pmp(W)
aSi	**805**	6.0	1997	**800**	6.0	1946	**750**	6.0	1833
CIS	350	**14**	**2262**	340	**14**	**2192**	320	**14**	**2008**
CIGS	350	12.2	1952	340	12.2	1881	320	12.2	1720
CdTe	370	9.7	1817	360	9.7	1779	350	9.7	1732

Figure 4.12 b:Values of Isc, Voc, Pmp at different conditions for shading pattern

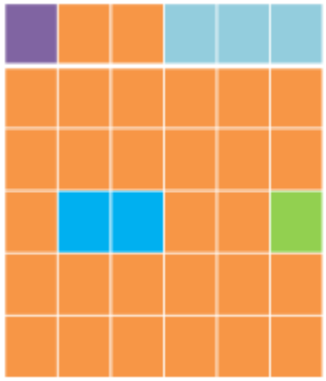

Figure 4.12 c:Pattern 4 with shading

Values of Isc , Voc , Pmp at different conditions for shading pattern 4									
Material	15 °C			25 °C			45 °C		
	Voc(V)	Isc(A)	Pmp(W)	Voc(V)	Isc(A)	Pmp(W)	Voc(V)	Isc(A)	Pmp(W)
aSi	**805**	6.3	2400	**800**	6.3	2334	**750**	6.3	2184
CIS	350	**15**	**2750**	340	**15**	**2629**	320	**15**	**2384**
CIGS	350	13	2356	340	13	2250	320	13	2042
CdTe	370	10	2284	360	10	2232	350	10	2130

Figure 4.12 d:Values of Isc, Voc, Pmp at different conditions for shading pattern 4

4.2 Results and discussion based on double Diode model

Let see the effect of Double Diode Model. The same circuit diagram but now we are using two diode model. The same four materials are now experimented with the same shading effect and temperature effects. The Voc is still decreasing of all four materials with increasing in temperature it can be seen in all three temperature graphs. The behavior of I-V curve without shading is almost same the only difference the Double Diode makes is a very slight bend in the curves of all materials without any changes in Voc and Isc. But due to addition of double the efficiency has increased which we will see in the next figure in P-V curve.

I-V Analysis of different Solar Cells using various materials without Shading at different temperature.

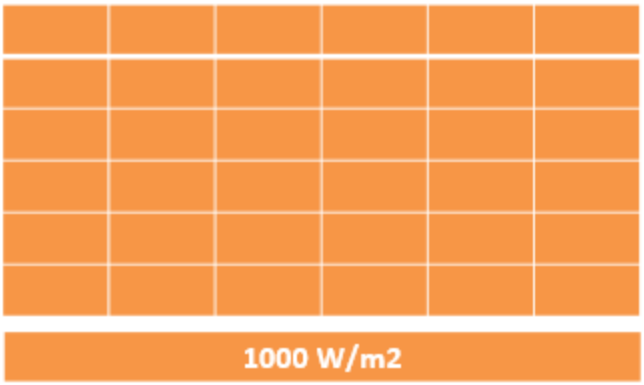

Figure 4.13 a:Pattern without shading

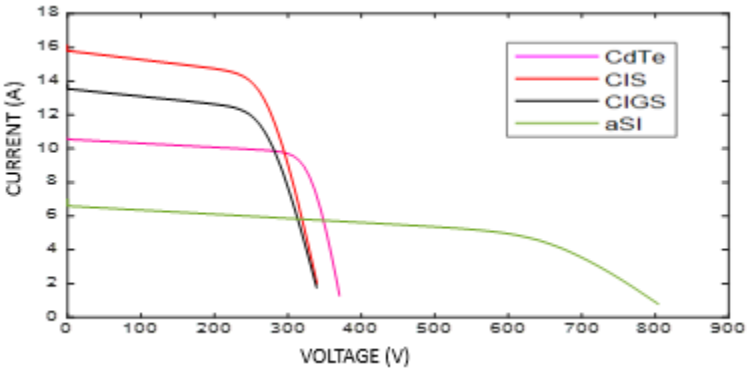

Figure 4.13 b:Current and Voltage graph at 15 ℃

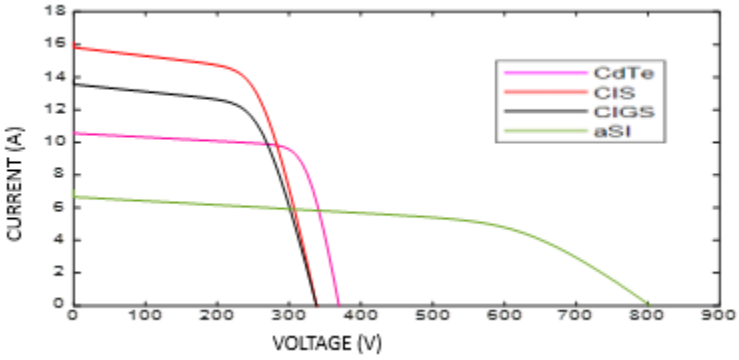

Figure 4.13 c:Current and Voltage graph at 25 ℃

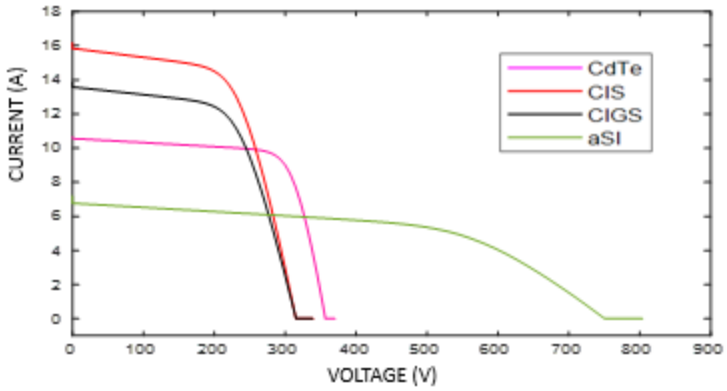

Figure 4.13 d:Current and Voltage graph at 45 ℃

Now in figure 4.14 we will see the P-V graph the same pattern without any shading. We can see power at maximum point of all four materials. But for Double diode as I already said that the efficiency is improved and hence it increases the maximum power of all four materials. Take a-SI as an example here if we see the maximum power at 15 C it is 2979 W. While the same if we compare with single Diode model at 15 C the a-SI has the maximum power of 2853W. Which is almost 126 W increase in power. This is because due to addition of double diode the efficiency of model gets increase and hence it generates more power as compared to single diode.

P-V Analysis of different Solar Cells using various materials without Shading at different temperature.

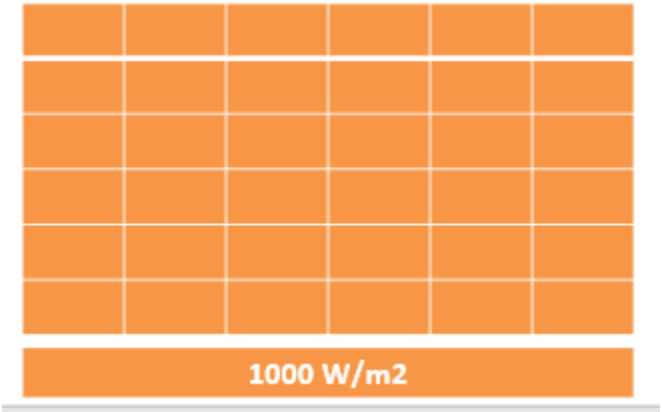

Figure 4.14 a:Pattern without shading

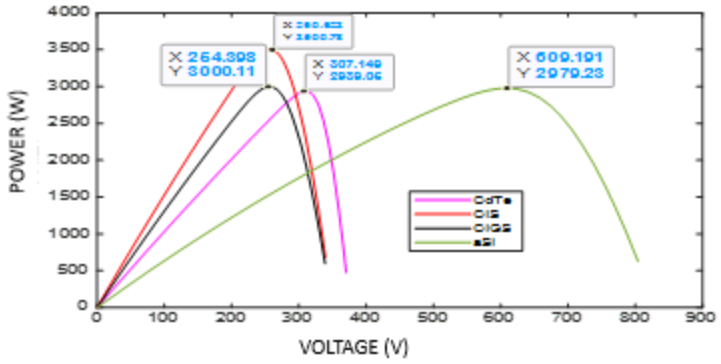

Figure 4.14 b:Power and Voltage graph at 15 ℃

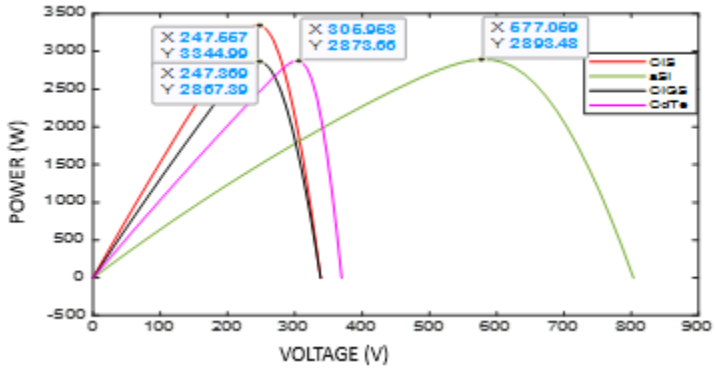

Figure 4.14 c:Power and Voltage graph at 25 ℃

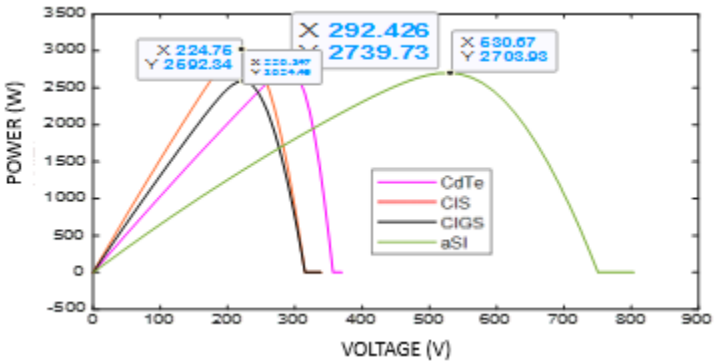

Figure 4.14 d:Power and Voltage graph at 45 ℃

Let's have a look on shading pattern. This is the first shading pattern in which light blue represent the shading of 800w/m2. The same effect has happened here as well the Short current is reduced due the shading at first two columns. As the current has neglected the path of shaded region and now moving in the unshaded region. So due to the decrease in strings the Short circuit current has reduced. So let's see the effect on power after parallel shading because that is our main aim.

I-V Analysis of different Solar Cells using various materials with Shading Pattern 1 at different temperature.

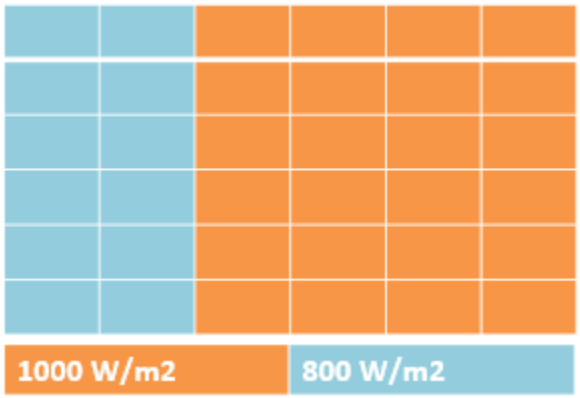

Figure 4.15 a:Pattern with shading

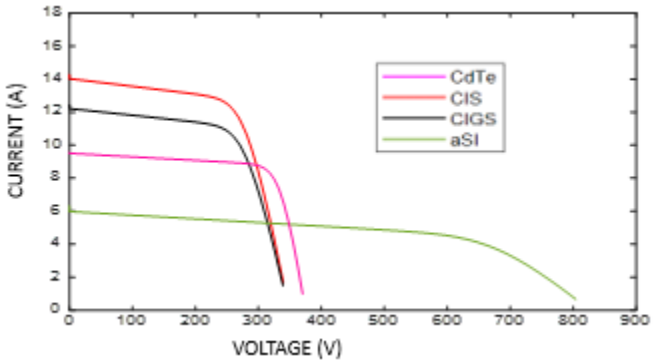

Figure 4.15 b:Current and Voltage graph at 15 ℃

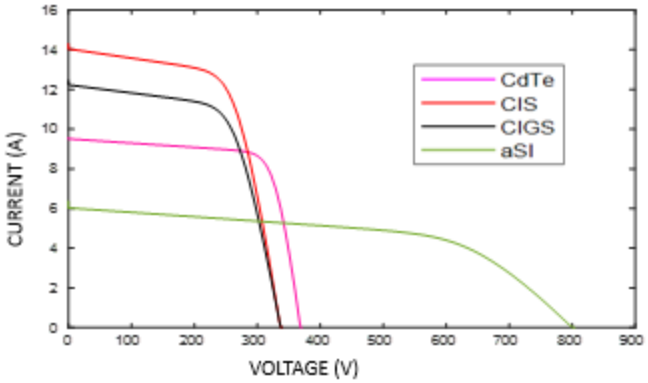

Figure 4.15 c:Current and Voltage graph at 25 ℃

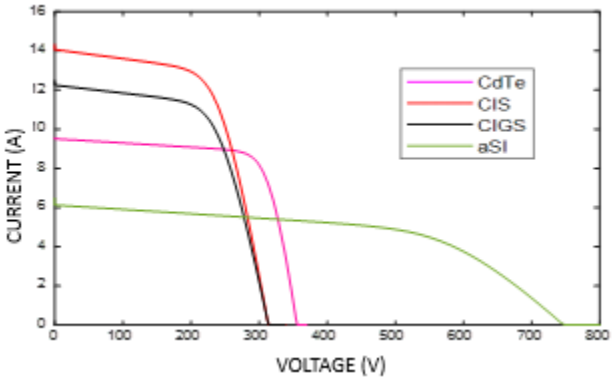

Figure 4.15 d:Current and Voltage graph at 45 ℃

The same shading pattern but we are seeing the P-V curve here now. Due to the addition of double diode the Power is relatively high as compared to Single Diode model. If we compare a power of both model for the same shading patterns than we can see a-SI at 15 C with double gives 2804W. While the a-SI at same temperature for single Diode gives 2722W which is low as compared to double diode model. That is the 82 W reduction in maximum power. Let's change the shading pattern to see the further effects. The effect is shown in below figure

P-V Analysis of different Solar Cells using various materials with Shading Pattern 1 at different temperature.

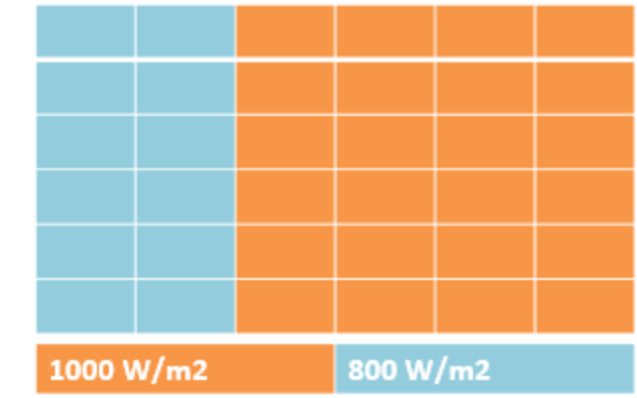

Figure 4.16 a:Pattern with shading

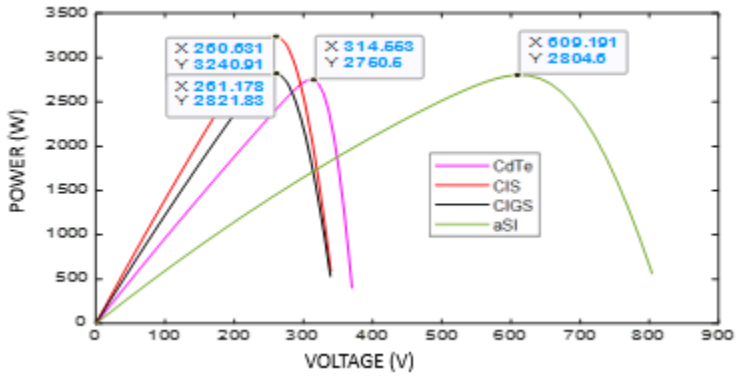

Figure 4.16 b:Power and Voltage graph at 15 ℃

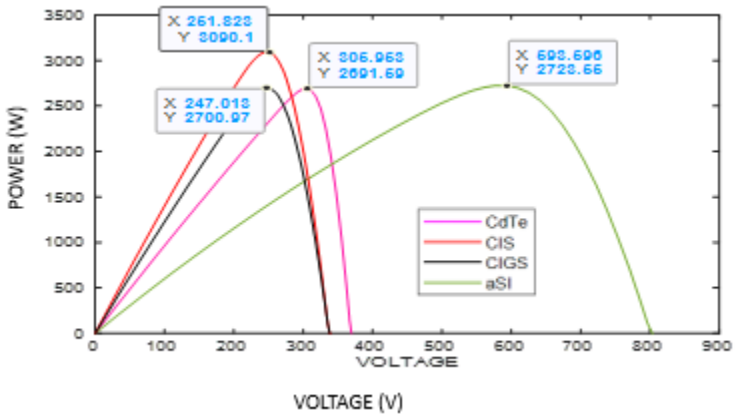

Figure 4.16 c:Power and Voltage graph at 25 ℃

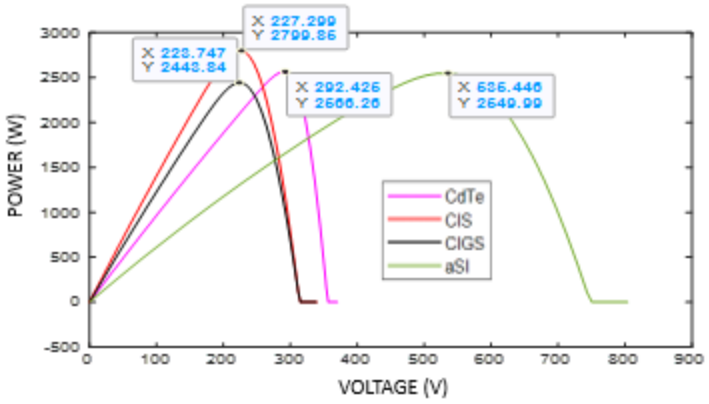

Figure 4.16 d:Power and Voltage graph at 45 ℃

Now the shading pattern 2 where last rows are shaded with 800w/m2. The steps can be seen in the curves and this due to the use of bypass diode. As it was previously seen in the single diode model that the shading at rows effects the reduction in the power more. So let's see how this shading effects the power.

I-V Analysis of different Solar Cells using various materials with Shading Pattern 2 at different temperature.

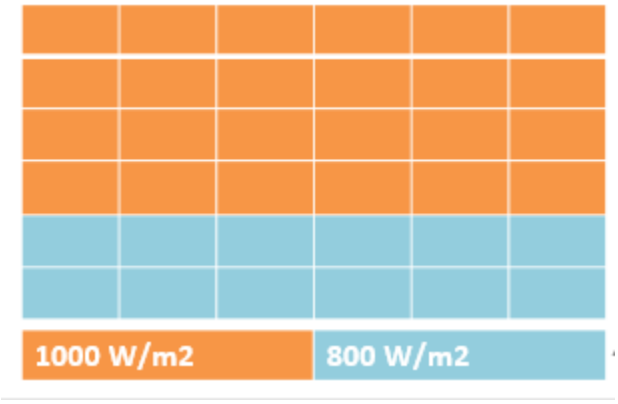

Figure 4.17 a:Pattern with shading

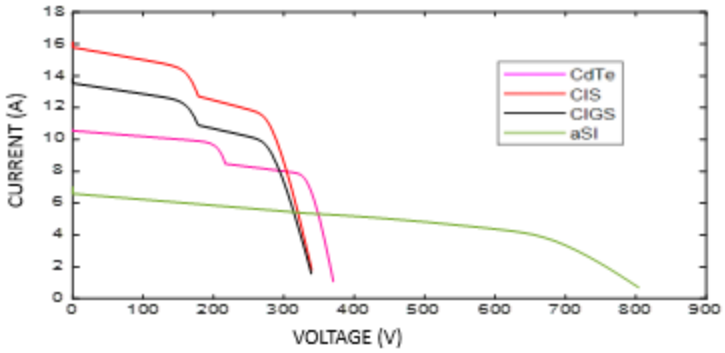

Figure 4.17 b:Current and Voltage graph at 15 ℃

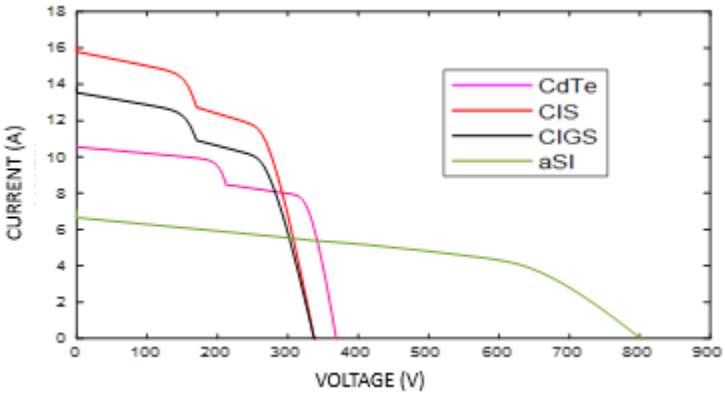

Figure 4.17 c:Current and Voltage graph at 25 ℃

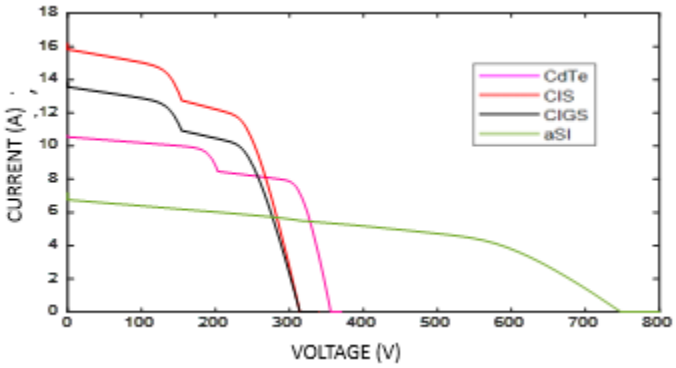

Figure 4.17 d:Current and Voltage graph at 45 ℃

The P-V graphs for the same shading pattern. Comparing a double diode model even for this shading as well with the Singe Diode we can see the a-SI has higher maximum power which is 2653W for 15 C but for single diode model it was 2524W. Its almost 4.86 % increase in maximum power. So we can see that Double diode is better than Single Diode in term of maximum power.

P-V Analysis of different Solar Cells using various materials with Shading Pattern 2 at different temperature.

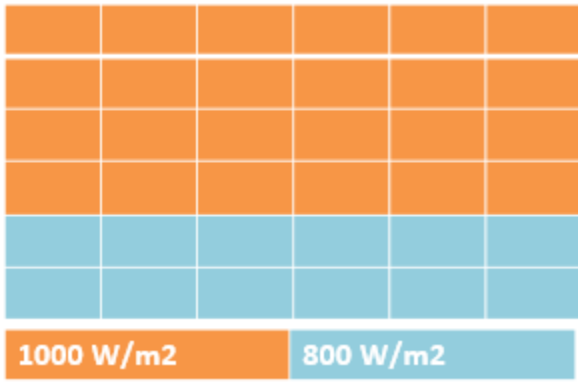

Figure 4.18 a:Pattern with shading

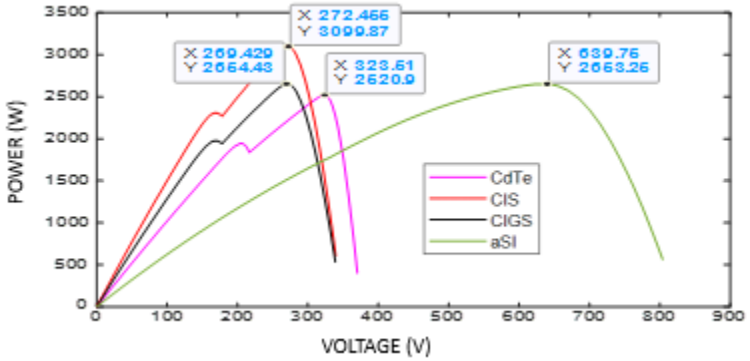

Figure 4.18 b:Power and Voltage graph at 15 ℃

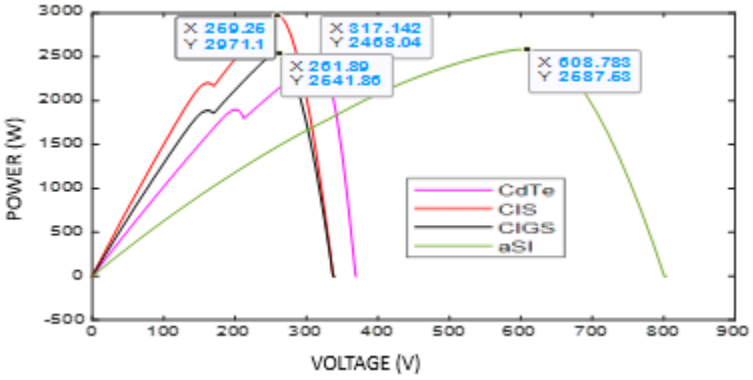

Figure 4.18 c:Power and Voltage graph at 25 ℃

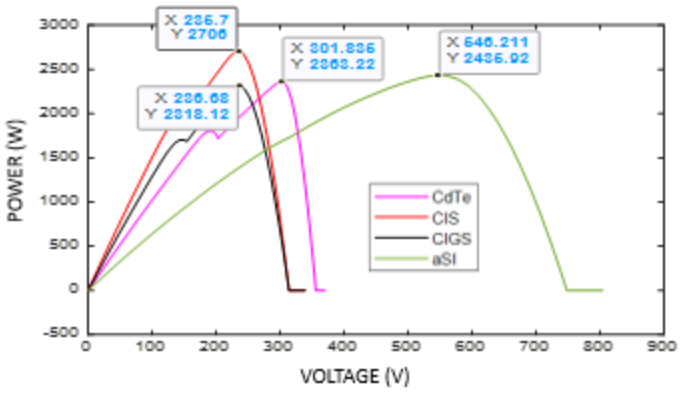

Figure 4.18 d:Power and Voltage graph at 45 ℃

The I-V curve of shading pattern 3. This is the highest shading pattern among all four pattern. And the reduction in short circuit current is due to shade in parallel strings as already discuss. And as we already said with the increase in shading the steps in the curves increases which effect the smoothness of the output curve.

I-V Analysis of different Solar Cells using various materials with Shading Pattern 3 at different temperature.

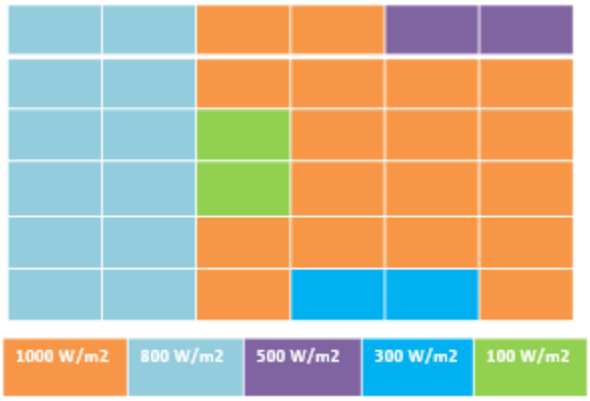

Figure 4.19 a:Pattern with shading

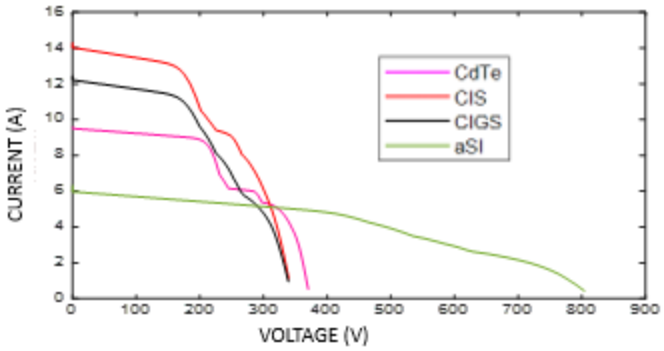

Figure 4.19 b:Current and Voltage graph at 15 ℃

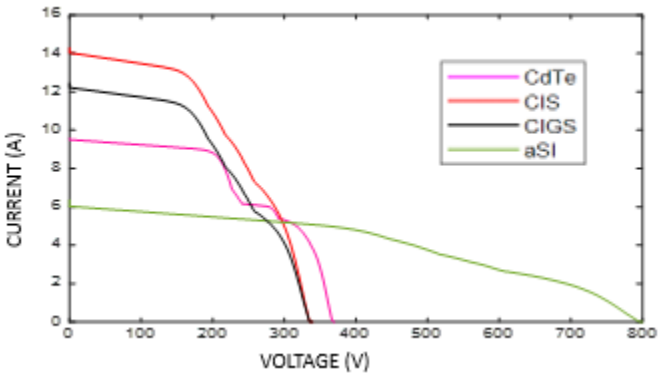

Figure 4.19 c:Current and Voltage graph at 25 ℃

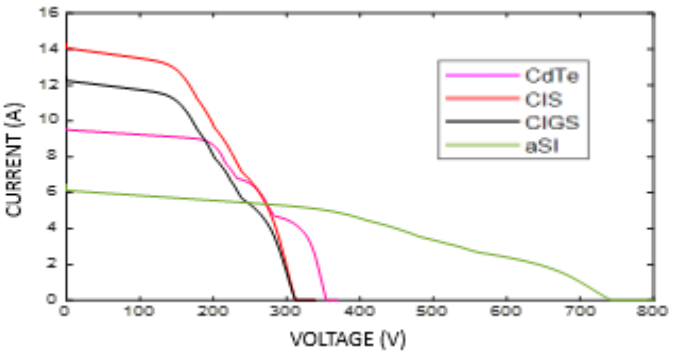

Figure 4.19 d:Current and Voltage graph at 45 ℃

P-V curve of this pattern 3. Now if we compare the maximum power of the same shading pattern with Single diode model. Than we can see the power of single diode model is less than the maximum power of double diode. For example, at 15 C the power of a-SI for Single diode for shading pattern 3 was 1997 W but here we have 2054W for double diode model which is almost 2.77 % higher than the single diode. Similarly, it is higher for remaining 2 graphs for 25 and 45 C.

P-V Analysis of different Solar Cells using various materials with Shading Pattern 3 at different temperature.

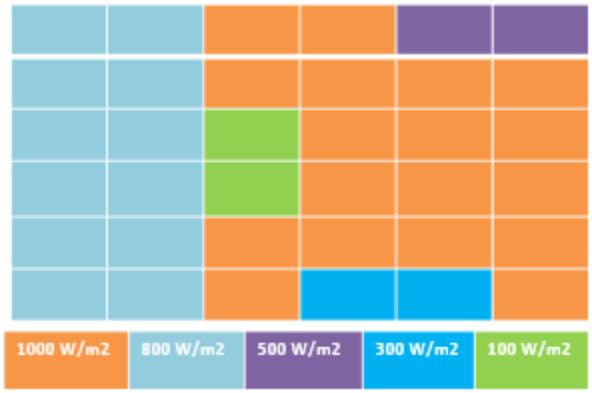

Figure 4.20 a:Pattern with shading

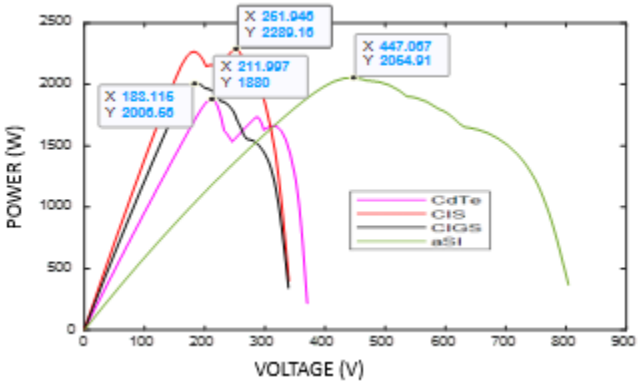

Figure 4.20 b:Power and Voltage graph at 15 ℃

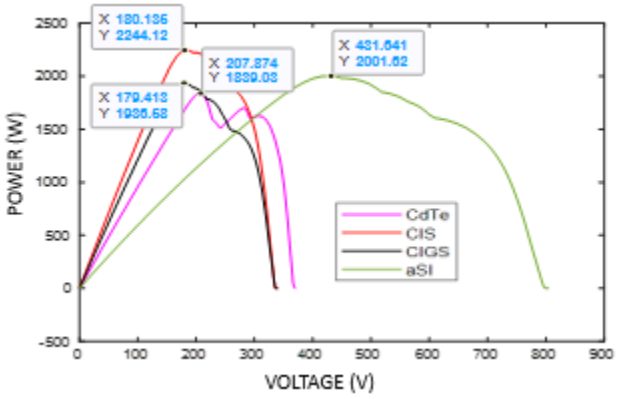

Figure 4.20 c:Power and Voltage graph at 25 ℃

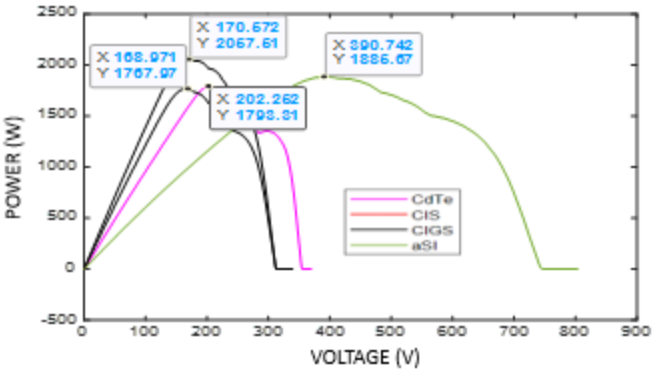

Figure 4.20 d:Power and Voltage graph at 45 ℃

Finally, the last shading pattern. Let's also compare the maximum power of this pattern to see the effect.

I-V Analysis of different Solar Cells using various materials with Shading Pattern 4 at different temperature.

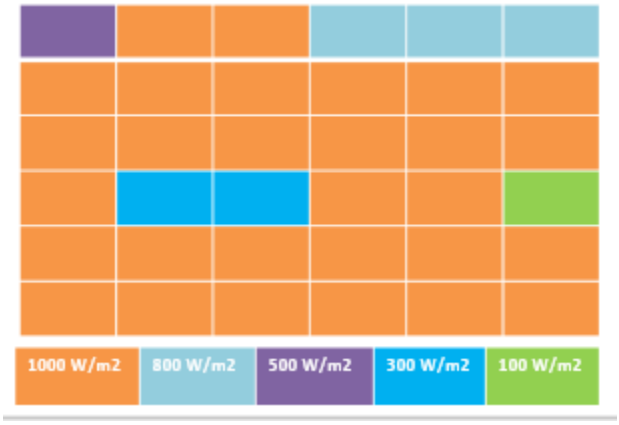

Figure 4.21 a:Pattern with shading

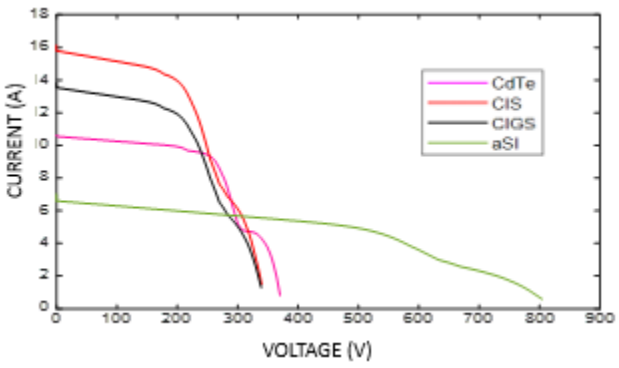

Figure 4.21 b:Current and Voltage graph at 15 ℃

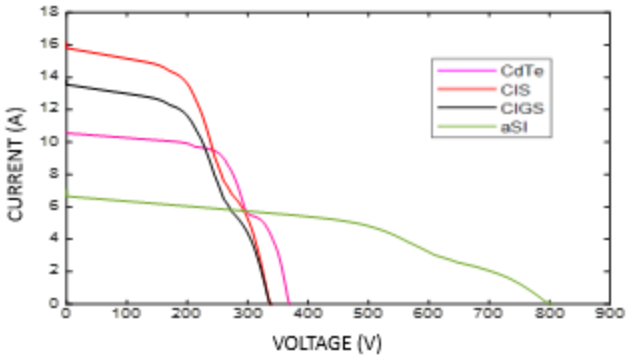

Figure 4.21 c:Current and Voltage graph at 25 ℃

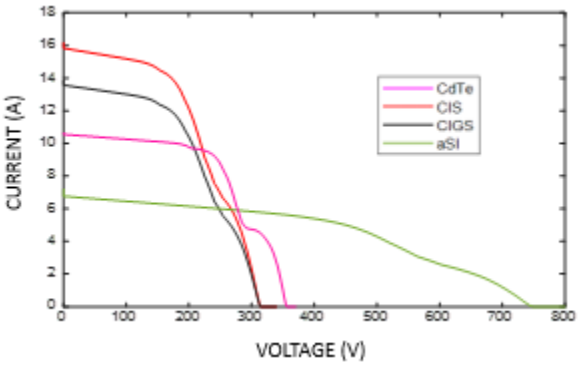

Figure 4.21 d:Current and Voltage graph at 45 ℃

P-V analysis of the last shading pattern. Comparing the final shading pattern with the Single diode of same shading pattern. We can see the power of amorphous silicon here at 15 C is 2481 W but with single diode it was 2400W. Which is 3.26 % higher so summarizing the all results we can say that Double diode has a better efficiency as compared to single.

P-V Analysis of different Solar Cells using various materials with Shading Pattern 4 at different temperature.

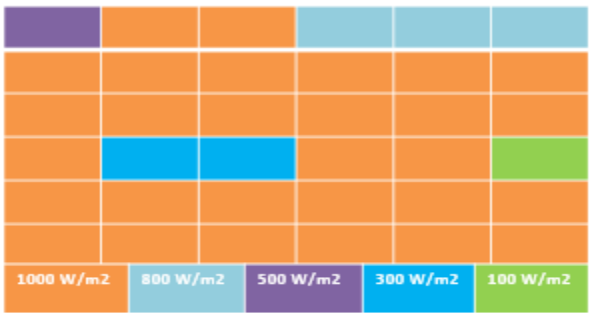

Figure 4.22 a:Pattern with shading

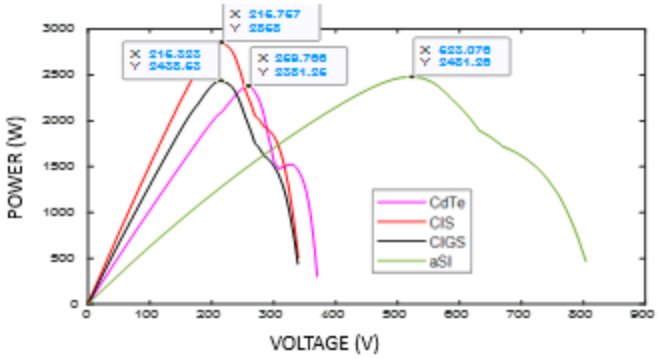

Figure 4.22 b:Power and Voltage graph at 15 ℃

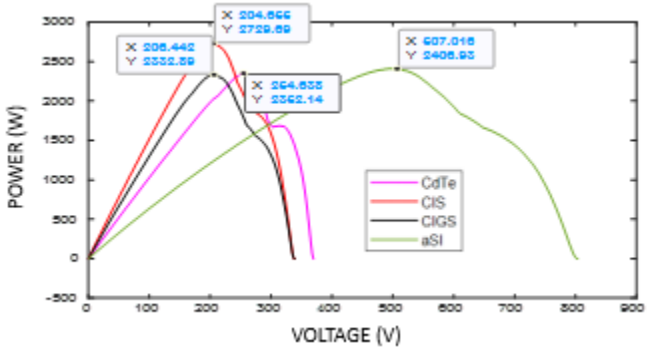

Figure 4.22 c:Power and Voltage graph at 25 ℃

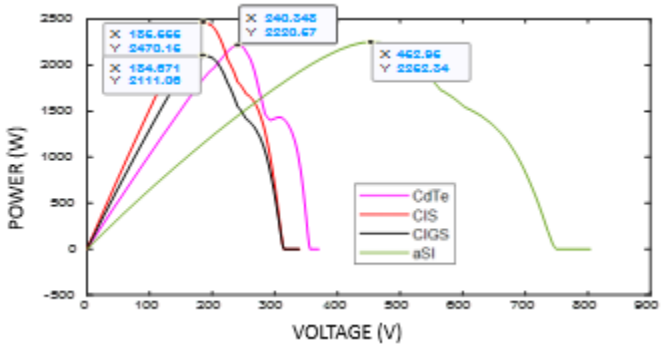

Figure 4.22 d:Power and Voltage graph at 45 ℃

Finally, the table which I have made using the I-V and P-V curves of Double Diode Model as the graphs are already shown above. So you can see the Amorphous silicon and CIS still exhibit good properties in Double Diode as well in term of Open Circuit Voltage Short Circuit Current and Power. It can be seen that the double diode gives more maximum power.

OBSERVATION FROM I-V AND P-V DATA FOR PATTERN 1 AND 2.

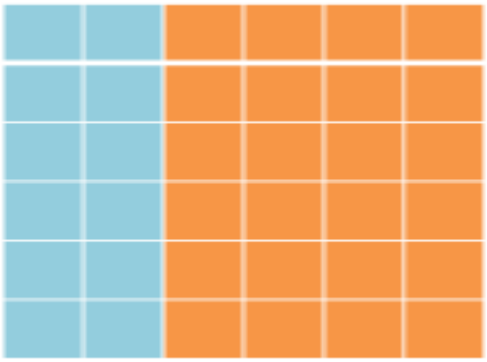

Figure 4.23 a:Pattern 1 with shading

Values of Isc , Voc , Pmp at different conditions for shading pattern 1									
Material	15 °C			25 °C			45 °C		
	Voc(V)	Isc(A)	Pmp(W)	Voc(V)	Isc(A)	Pmp(W)	Voc(V)	Isc(A)	Pmp(W)
aSi	**805**	6.0	2804.6	**800**	6.0	2723.5	**750**	6.0	2549.9
CIS	350	**14**	**3240.9**	340	**14**	**3090.1**	320	**14**	**2799.8**
CIGS	350	12.2	2821.8	340	12.2	2700.9	320	12.2	2443.8
CdTe	370	9.7	2750.5	360	9.7	2691.5	350	9.7	2566.2

Figure 4.23 b:Values of Isc, Voc, Pmp at different conditions for shading pattern 1

Figure 4.23 c:Pattern 2 with shading

Values of Isc , Voc , Pmp at different conditions for shading pattern 2									
Material	15 °C			25 °C			45 °C		
	Voc(V)	Isc(A)	Pmp(W)	Voc(V)	Isc(A)	Pmp(W)	Voc(V)	Isc(A)	Pmp(W)
aSi	**805**	6.3	2653.2	**800**	6.3	2587.5	**750**	6.3	2435
CIS	350	**15**	**3099.8**	340	**15**	**2971.1**	320	**15**	**2706**
CIGS	350	13	2654.4	340	13	2541.8	320	13	2318.1
CdTe	370	10	2520.9	360	10	2468.0	350	10	2363.2

Figure 4.23 d:Values of Isc, Voc, Pmp at different conditions for shading pattern 2

These are the pattern 3 and 4 and using the I-V and P-V curve of 3 and 4 pattern I have made these two tables. Similarly, for Pattern 3 & 4 if we compare the power of CIS at 15 C for Pattern 4 of Double Diode which 2858W but for single Diode model it was 2750W which is 3.77% increase so here we can say that in the Double Diode model the efficiency of the system is better than in case of single diode model.

OBSERVATION FROM I-V AND P-V DATA FOR PATTERN 3 AND 4.

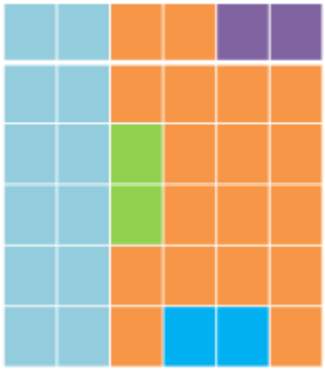

Figure 4.24 a:Pattern 3 with shading

Values of Isc , Voc , Pmp at different conditions for shading pattern 3									
Material	15 °C			25 °C			45 °C		
	Voc(V)	Isc(A)	Pmp(W)	Voc(V)	Isc(A)	Pmp(W)	Voc(V)	Isc(A)	Pmp(W)
aSi	**805**	6.0	2054.9	**800**	6.0	2001.6	**750**	6.0	1885.6
CIS	350	**14**	**2289**	340	**14**	**2244.1**	320	**14**	**2057**
CIGS	350	12..2	2006.5	340	12.2	1936.5	320	12.2	1767.9
CdTe	370	9.7	1880	360	9.7	1839	350	9.7	1793.3

Figure 4.24 b:Values of Isc, Voc, Pmp at different conditions for shading pattern 3.

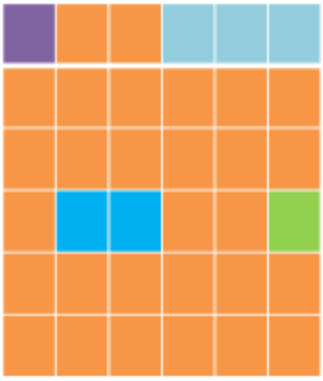

Figure 4.24 c:Pattern 4 with shading

Figure 4.24(c): Pattern 4 with shading

Values of Isc , Voc , Pmp at different conditions for shading pattern 4									
Material	15 °C			25 °C			45 °C		
	Voc(V)	Isc(A)	Pmp(W)	Voc(V)	Isc(A)	Pmp(W)	Voc(V)	Isc(A)	Pmp(W)
aSi	**805**	6.3	2481.2	**800**	6.3	2406	**750**	6.3	2352
CIS	350	**15**	**2858**	340	**15**	**2729**	320	**15**	**2470**
CIGS	350	13	2438	340	13	2332.8	320	13	2111
CdTe	370	10	2381	360	10	2352	350	10	2220.5

Figure 4.24 d:Values of Isc, Voc, Pmp at different conditions for shading pattern 4.

CHAPTER 5:

CONCLUSION AND FUTURE WORK

5.1 Conclusion

Materials with low band gap give comparatively high current and low voltage, while materials with high band gap give low current and high voltage. In the case of CdTe when cell temperature increases by 1°C above 25°C, Voc decreases by 0.13% Where MPP slides toward left by 0.13%. In the case of a-Si, when cell temperature increases by 1°C above 25°C, Voc decreases by 0.31% Where MPP slides towards left by 0.5%. The band gap of a-Si is 1.75 eV which is quite higher than optimal value i.e. 1.44 eV, which increases the voltage and lower the current among all four materials.

Reflection losses of CdTe is 32% therefore the extracted output power is approximately 6.28% less than that of CIGS for low temperature. CdTe has a high temperature stability, change in temperature has a less effect on output voltage as compared to other materials.

5.2 Future Work

While designing a PV solar system, some shadowing is unavoidable due to space limitation and high vertical infrastructure. In order to achieve the highest yields. If defined shadows are to be expected, (for example: horizontal shadows in the morning or evening cast by a shed roof, or in a field system), then energy production can be optimized by installing PV module of appropriate materials. Double Diode Model should be preferred due to the fact that; the maximum power reduces in a less amount with instantaneous variation in irradiance.

MPPT controller can work better in the case of a-Si due to less local peaks in the P-V and I-V curve. For the high current application area CIS is recommended. For high voltage application a-Si material is recommended. For the limited installation area where cloud cover is of average 7 to 8 hours per week a-Si is preferred for the limited installation area where cloud cover is of average 15 to 16 hours per week CIS is preferred.

Bibliography

[1] "World bank report "Global Photovoltaic Power Potential by Country",," 2020.

[2] A. A. R. I. A. J. M. a. G. S. Ul-Haq, " Computation of power extraction from photovoltaic arrays under various fault conditions. IEEE Access, 8, pp.47619-47639.," , 2020..

[3] G. G. S. E. B. A. F. A. F. a. I. T. Seritan, "Performance Evaluation of a Partially Shaded PV cell with Different Bus Bars Configurations. In 2019 54th International Universities Power Engineering conferance (UPEC)," , 2019, September..

[4] M. C. V. M. S. a. S. Z. Kermadi, "A fast and accurate generalized analytical approach for PV arrays modeling under partial shading conditions. Solar Energy, 208, pp.753-765.," 2020. .

[5] C. R. C. B. R. a. O. S. Hussaian Basha, "Simulation of metaheuristic intelligence MPPT techniques for solar PV under partial shading condition. In Soft Computing for Problem Solving (pp. 773-785). Springer, Singapore.," , 2020. .

[6] Z. a. M. Y. Alqaisi, "Comprehensive study of partially shaded PV modules with overlapping diodes. IEEE Access, 7, pp.172665-172675.," , 2019. .

[7] P. S. R. P. S. a. P. S. Satpathy, "Bypass diodes configurations for mismatch and hotspot reduction in PV modules. In 2020 International Conference on Computational Intelligence for Smart Power System and Sustainable Energy.," 2020, July.

[8] K. B. A. C. a. S. S. M. Tadj, "``Improving the performance of PV systems by faults detection using GISTEL approach," Energy Convers. Manage., vol. 80, pp. 298304,," Apr. 2014,.

[9] Y. S. B. T. A. S. a. M.-E. H. F. Harrou, "``Reliable fault detection and diagnosis of photovoltaic systems based on statisticalmonitoring approaches," Renew. Energy, vol. 116, pp. 2237, doi: 10.1016/j.renene.2017.09.048.," Feb. 2018, .

[10] J. SolÓrzano and M. Egido, " ``Automatic fault diagnosis in PV systems with distributed MPPT," Energy Convers. Manage., vol. 76, pp. 925934,, doi: 10.1016/j.enconman.2013.08.055.," Dec. 2013.

[11] K. K. A. C. S. S. a. S. K.] E. Garoudja, ", ``Efcient fault detection and diagnosis procedure for photovoltaic systems," in Proc.8th Int. Conf. Modelling, Identicat. Control (ICMIC), Algiers, Algeria,, pp. 851856, doi: 10.1109/I," 2016.

[12] T. N. T. J. M. L. R. a. F. F. C. Alves, " Different Techniques to Mitigate Partial Shading in Photovoltaic Panels. Energies, 14(13), p.3863.," 2021..

[13] H. S. Sahu and S. K. Nayak, " ``Extraction of maximum power from a PV array under nonuniform irradiation conditions," IEEE Trans. Electron Devices, vol. 63, no. 12, pp. 48254831, doi: 10.1109/ ted.2016.2616580," Dec. 2016, .

[14] A. R. A. E. H. a. M. D. M. Davarifar, " ``New method for fault detection of PV panels in domestic applications," presented at the 4th Int. Conf. Smart Cities Green ICT Syst.,," 2013.

[15] G. M. Master., "Renewable and Efficient Electric Power systems written by Gilbert M. Master.".

[16] A. K. a. M. Saad, ", "Analysis of multi-crystalline silicon solar cells at low illumination level," 2010.

[17] F. a. O. H. Bayrak, ". Effects of static and dynamic shading on thermodynamic and electrical performance for photovoltaic panels. Applied Thermal Engineering, 169, p.114900.," , 2020.

[18] T. N. T. J. M. L. R. a. F. F. C. Alves, "Different Techniques to Mitigate Partial Shading in Photovoltaic Panels. Energies, 14(13), p.3863.," , 2021. .

[19] A. B. M. J. V. F. a. A. C. Gutiérrez Galeano, "Shading ratio impact on photovoltaic modules and correlation with shading patterns. Energies, 11(4), p.852.," 2018. .

[20] G. E. B. A. F. A. F. C. C. V. V. T. A. G. C. a. H. F. Seritan, " Performance evaluation of photovoltaic panels containing cells with different bus bars configurations," 2020..

[21] A. R. H. a. Y. D. Fathy, " A robust global MPPT to mitigate partial shading of triple-junction solar cell-based system using manta ray foraging optimization algorithm. Solar Energy, 207, pp.305-316.," 2020..

[22] M. C. V. M. S. a. S. Z. Kermadi, " A fast and accurate generalized analytical approach for PV arrays modeling under partial shading conditions. Solar Energy, 208, pp.753-765.," 2020..